Univerzita Palackého v Olomouci

Přírodovědecká fakulta

Katedra fyzikální chemie

Analýza neurotransmiterů pomocí povrchem zesílené Ramanovy spektroskopie

Diplomová práce

Autor:	Bc. Klára Gajdošová
Vedoucí práce:	Mgr. Zuzana Chaloupková, Ph.D.
Konzultant:	doc. RNDr. Václav Ranc, Ph.D.

Studijní program:	Chemie
Studijní obor:	Materiálová chemie
Forma studia:	Prezenční

Palacký University Olomouc

Faculty of Science

Department of Physical Chemistry

Analysis of Neurotransmitters Using Surface Enhanced Raman Spectroscopy

Diploma Thesis

Author:	Bc. Klára Gajdošová
Supervisor:	Mgr. Zuzana Chaloupková, Ph.D.
Consultant:	doc. RNDr. Václav Ranc, Ph.D.

Study programme:	Chemistry
Study major:	Material chemistry
Study form:	Full-time

I hereby declare that I have written this diploma thesis myself, it is based on my research, and I have cited each source used for this work in bibliography.

In Olomouc:

Klára Gajdošová

Acknowledgements

I would like to thank the supervisor of this work, Mgr. Zuzana Chaloupková, Ph.D., for her guidance, support, and patience. Thank you for teaching me how to operate Raman spectroscope, process data, and for being positive and making me feel welcome.

I would also like to thank doc. RNDr. Václav Ranc, Ph.D. for enabling this project and acquiring brain tissue from the Faculty of Medicine in Olomouc, and his help with data processing. His advice and insight into the topic were greatly valued.

I also thank Mgr. Zdenka Medříková, Ph.D. for synthesising and characterising the magnetic nanocomposite used in this work.

Bibliografická identifikace

Autor:	Klára Gajdošová
Název práce:	Analýza neurotransmiterů pomocí povrchem zesílené Ramanovy spektroskopie
Typ práce:	Diplomová
Pracoviště:	Regionální Centrum Pokročilých Technologií a Materiálů (RCPTM), Český Institut pokročilých technologií a výzkumu (CATRIN), Univerzita Palackého v Olomouci (UPOL)
Vedoucí práce:	Mgr. Zuzana Chaloupková, Ph.D.
Konzultant:	doc. RNDr. Václav Ranc, Ph.D.
Rok obhajoby:	2021
Abstrakt:	Cílem této práce bylo ověřit možnost aplikace magnetického nanokompozitu k detekci neurotransmiterů dopaminu a serotoninu pomocí magneticky asistované povrchem zesílené Ramanovy spektroskopie. V sadách provedených experimentů byly hledány nejvhodnější podmínky pro detekci anebo kvantifikaci obou látek. Detekce byla nejprve prováděna z vodného roztoku, poté z roztoku připraveného v PBS pufru, a nakonec z umělého mozkomíšního moku (aCSF). V roztocích PBS a aCSF byla připravena sada vzorků obsahujících dopamin i serotonin v různých vzájemných poměrech, a to až v desetinásobku jednoho z neurotransmiterů. Pak byla provedena jejich simultánní detekce, což bylo ověřeno diskriminační analýzou. Na základě předchozích měření byla pro obě látky sestavena kalibrační křivka v aCSF a stanoveny limity detekce. Ty jsou za uvedených podmínek 1,82 μM pro dopamin a 0,04 mM pro serotonin. Na závěr byla MA-SERS metoda aplikovaná na extrakt z mozkové tkáně striata myší.
Klíčová slova:	dopamin, serotonin, magneticky asistovaná povrchem zesílená Ramanova spektroskopie (MA-SERS), magnetický nanokompozit
Počet stran:	51
Počet příloh:	1
Jazyk:	Anglický

Bibliographic Identification

Author:	Klára Gajdošová
Title:	Analysis of Neurotransmitters Using Surface Enhanced Raman Spectroscopy
Type of Thesis:	Diploma
Department:	Regional Centre of Advanced Technologies and Materials (RCPTM), Czech Advanced Technology and Research Institute (CATRIN), Palacký University Olomouc (UPOL)
Supervisor:	Mgr. Zuzana Chaloupková, Ph.D.
Consultant:	doc. RNDr. Václav Ranc, Ph.D.
The Year of Presentation:	2021
Abstract:	The goal of this work was to examine the possibility of applying magnetic nanocomposite for label-free detection of neurotransmitters dopamine and serotonin using magnetically assisted surface enhanced Raman spectroscopy. The best conditions for detecting or quantifying these substances were explored. Neurotransmitters were detected from an aqueous solution, PBS solution, and artificial cerebrospinal fluid (aCSF). In PBS and aCSF samples, a set of mixtures was prepared, containing up to 10fold of one neurotransmitter. Simultaneous analysis was performed, which was proved by discriminant analysis. Later, calibration curves were assembled, and respective limits of detection (LOD) calculated. LOD for dopamine was 1.82 μM and for serotonin 0.04 mM. Lastly, MA-SERS detection was applied on an extract from mouse brain tissue striatum.
Keywords:	dopamine, serotonin, magnetically assisted surface enhanced Raman spectroscopy (MA-SERS), magnetic nanocomposite
Number of Pages:	51
Number of Appendices:	1
Language:	English

TABLE OF CONTENTS

1 INTRODUCTION

Neurotransmitters are important molecules located in the brain tasked with signalling various physiological or behavioural functions. Dopamine, for instance, is responsible for functions including motor control, attention, motivation, and reward.[1,2] Consequently, its dysfunctions are correlated with several neuropsychiatric disorders such are Parkinson's disease[1], addiction[3], major depressive disorder[2], or schizophrenia[4]. Serotonin is involved in controlling appetite, circadian rhythm, aggression, and sexual behaviour[5], among other functions. Disruptions of neuronal serotoninergic system can lead to major depressive disorder[2], eating disorders[6], or a group of anxiety disorders[7].

Neurotransmitters are conventionally analysed by chromatographic methods coupled with mass spectrometric detection[8], or by cyclic voltammetry[9]. Although these techniques allow physiological limit of detection, they are either time consuming or not selective enough. Surface enhanced Raman spectroscopy (SERS) is a powerful method that has the potential to substitute previously mentioned techniques.

SERS detection of both dopamine and serotonin at physiological levels was previously achieved using different signal enhancing platforms.[10,11] Their simultaneous detection however was executed only four times so far, and only in aqueous solutions.[12–15]

In this work, magnetic nanocomposite with silver nanoparticles was employed as the signal enhancing platform. Its magnetic core allowed simple analyte separation from a complex matrix and its preconcentration before measurement. The goal of this work was applying magnetically assisted surface enhanced Raman spectroscopy (MA-SERS) for the detection of one or both neurotransmitters dopamine and serotonin dissolved in biologically relevant matrix such are PBS solution and artificial cerebrospinal fluid. MA-SERS detection of dopamine and serotonin was also successfully tested on an extract from mouse brain tissue striatum. Simultaneous label-free detection of dopamine and serotonin was achieved in PBS solution and artificial cerebrospinal fluid. Several ratios of respective neurotransmitters were tested, up to 10fold abundance. Lastly, calibration curves were assembled for aCSF solutions with respective limits of detection.

2 THEORETICAL PART

2.1 Neurotransmitters

There are various groups of molecules in our bodies that enable us to function correctly. Neurotransmitters are a group of substances that transfer information in the brain, hence their name. Their function varies greatly and is enabled by neurotransmission from a neuron into synaptic cleft and its effect on specific receptors.[16] In the following chapters, neurotransmitters dopamine and serotonin are described.

2.1.1 Biochemistry and Function of Dopamine

Dopamine (DA), in organic chemistry nomenclature 3,4-dihydroxyphenylethylamine, is a member of the catecholamine group, which also includes noradrenaline and adrenaline.[17] It is synthesised from the essential amino acid L-phenylalanine (L-PHE) or the non-essential amino acid L-tyrosine (L-TYR), through L-DOPA (L-dihydroxyphenylalanine), as can be seen in Fig. 1A. This process is enabled by enzymes phenylalanine hydroxylase (PAH), tyrosine hydroxylase (TH), and DOPA decarboxylase (DDC).[18] The synthesis takes place in dopaminergic neuron terminals, in cytoplasm.[1] Dopamine is later released into the synaptic cleft, where it inhibits its own synthesis and/or release through interaction with autoreceptors (receptors located on a neuron that are sensitive to the transmitter released from said neuron).[19]

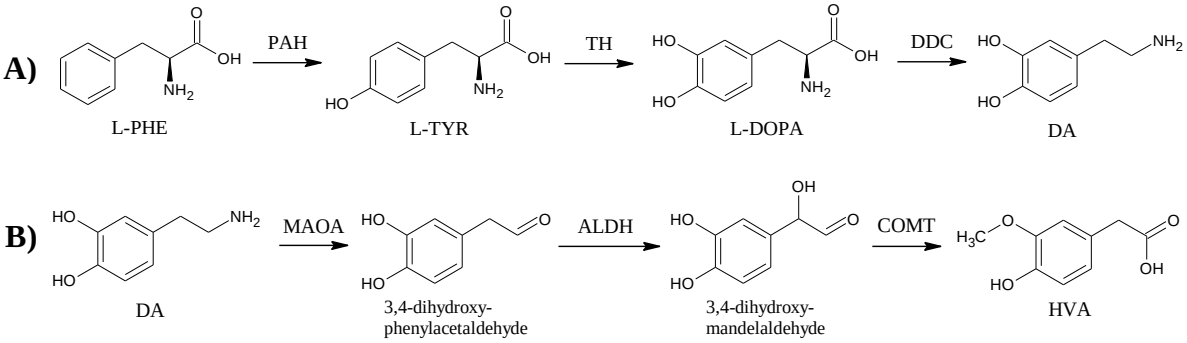

Fig. 1: *Metabolism of dopamine* ***A)*** *Synthesis of dopamine; L-PHE is L-phenylalanine, L-TYR L-tyrosine, L-DOPA L-dihydroxyphenylalanine, PAH phenylalanine hydroxylase, TH tyrosine hydroxylase, and DDC is DOPA decarboxylase* ***B)*** *Dopamine degradation; HVA is homovanillic acid, MAOA monoamine oxidase, ALDH aldehyde dehydrogenase, and COMT catechol-O-methyl transferase.*

Dopamine degradation pathway takes place in the presynaptic neuronal terminals[1] and is enabled by different enzymes, namely monoamine oxidase (MAOA), aldehyde dehydrogenase (ALDH), and catechol-O-methyl transferase (COMT). These enzymes degrade dopamine into homovanillic acid (HVA) (Fig. 1B).[18] HVA travels to kidneys through blood and is excreted from the body.[1]

Dopamine is one of the most important neurotransmitters of the central nervous system (CNS). It plays a significant role in the initiation of movement, attention, arousal, motivation, and emotions. Its actions are regulated through dopamine receptors (types D_1 – D_5). There are four to five dopaminergic networks: **1)** the nigrostriatal system (contains 70% of brain dopamine, responsible for motor control), **2)** the mesocortical system (responsible for motivation, concentration, and emotional response), **3)** the mesolimbic system (its neurons send axons to the ventral striatum, is responsible for reward, desire, and pleasure), **4)** the tuberoinfundibular system (responsible for secretion of hormone prolactin), and **5)** the incertohypothalamic system (sexual behaviour).[1,2]

Dopamine degrades in neutral or alkaline aqueous solutions due to reaction with dissolved oxygen.[20] The main products are hydrogen peroxide (H_2O_2) and dopamine orthoquinone, where superoxide serves as a chain-propagating radical in the autoxidation of dopamine[21] (reaction scheme in Fig. 2[22]). The oxidation can be catalysed by trace amount of transitional metals present in the solution.[21] This can be avoided by adding EDTA, which can inhibit such metals by binding them into a complex.[20]

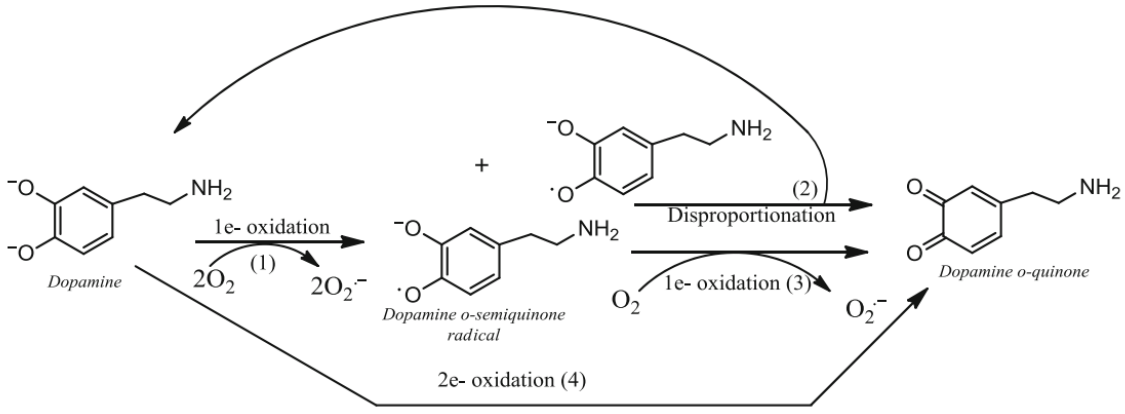

***Fig. 2**: Oxidation of dopamine by oxygen*[22]

The oxidation of dopamine by oxygen was further researched by *Sánchez-Rivera et al.*[23]. They showed, by measuring UV/VIS absorption spectra, that dopamine solution is degraded not only by oxygen, but also by exposure to light. Dopamine kept under N_2 atmosphere and without exposure to light was significantly more stable than dopamine

solution saturated with O_2 gas and/or with exposure to light. The experiments were performed at pH 3, 9 and 12, and dopamine's instability increased as a function of the pH.

Milovanović et al.[24] performed theoretical experiments using first principle molecular dynamics based on density functional theory (DFT) and the BLYP functional. They tracked oxidation of dopamine in aqueous solution caused by hydroxyl, peroxyl or methoxy radicals, trying to clarify the reaction mechanisms. For the case of oxidation by hydroxyl radical, the reaction followed PCET mechanism (proton-coupled electron transfer) when the radical was in dopamine's vicinity, and MS-PCET mechanism (multi-site proton-coupled electron transfer) when the radicals were relatively far away (more than 4.5 Å).

2.1.2 Brain Diseases Associated with Abnormal Levels of Dopamine

Dopamine is a vital neurotransmitter whose imbalance plays an important role in various diseases including Parkinson's disease, major depressive disorder, addictions, and schizophrenia.

The loss of dopaminergic neurons in the nigrostriatal pathway causes resting tremor in patients diagnosed with Parkinson's disease. It is a neurodegenerative disease afflicting mostly older members of the population. The motor symptoms can be treated by drugs containing L-DOPA (dopamine precursor) or D_2 receptor agonists. Parkinson's disease can be accompanied by depression, another illness where dopamine plays a role.[1,25]

Major depressive disorder's main symptom is anhedonia – the inability to experience pleasure. Depressed person moves protractedly, cannot concentrate, loses their interests, motivation, and energy. All the beforementioned symptoms are correlated with the overall reduction of dopamine and serotonin release. Drugs used for the treatment of depression that increase dopamine neurotransmission are e.g. from the group of MAOIs (monoamine oxidase inhibitors; target DA, serotonin, and norepinephrine), TCAs (tricyclic antidepressants), or SSRIs (selective serotonin reuptake inhibitors, at high doses prevent DA reuptake).[2]

The mesolimbic dopaminergic pathway, as mentioned before, is responsible for feelings of reward. Acute drug (self)administration increases dopamine levels on this pathway by lowering DA transporters and DA receptors availability. This may lead to development of addictions through changes in mesolimbic neuroplasticity. Such

response is induced by e.g., psychostimulant drugs (cocaine, amphetamine, and methamphetamine), opioids, nicotine, or ethanol.[3,26]

A complex psychiatric disorder whose pathophysiology is still not clear, but is certainly connected to alterations in dopamine levels, is schizophrenia. Currently, there is the third version of dopamine hypothesis of schizophrenia, especially its symptom psychosis, composed by *Howes and Kapur*.[27] They put together recent findings from almost 200 studies investigating the dopamine hypothesis by different methodology, including assessing risk factors, genetics, and brain tissue alterations. They conclude that patients with schizophrenia have excessive dopamine presynaptic neurotransmission in striatum. It is important to note that although the dopamine hypothesis is comprehensive and current medication for schizophrenia is based on it (blocks DA system, beneficial for psychosis), it does not explain all the symptoms of schizophrenia.[4,27,28]

2.1.3 Biochemistry and Function of Serotonin

Another important neurotransmitter with somewhat similar role as dopamine is serotonin (SE, 5-hydroxytryptophan, 5-HT). The uttermost amount of serotonin is localized in the gastrointestinal (GI) tract. Serotonin is synthesized in both the GI tract and the CNS from the essential amino acid tryptophan (TRP) by the effect of two enzymes – tryptophan hydroxylase (TPH) and aromatic amino acid decarboxylase (AADC) (Fig. 3A). The rate of its synthesis is governed by TRP availability.[29] 5-HT is stored in vesicles or granules, therefore protected from the enzyme monoamine oxidase (MAO) that degrades it. The main product of serotonin degradation is 5-hydroxyindoleacetic acid (5-HIAA) (Fig. 3B).[30]

As implied before, serotonin is an important molecule on the brain-gut axis. In the GI tract, serotonin influences e.g. secretion, perception of pain, and nausea.[31] In CNS, most serotoninergic neurons are located in the raphe nuclei. Their axons reach to various brain regions such are hypothalamus, cortex, hippocampus, amygdala, and striatum.[5]

Serotoninergic neurons activity differs during the day – most activity is observed in the awake state, medium activity in slow-wave sleep state, an no activity in the REM sleep state.[5]

There are seven subtypes of serotonin receptors (5-HT_1 – 5-HT_7) either in the CNS and/or the GI tract[31] through which serotonin regulates multiple functions. Neural serotonin regulates behavioural functions such are appetite and feeding, circadian

rhythm, sensorimotor reactivity, perception of pain, learning, aggression, substance abuse, and sexual behaviour.[5] This variety suggests serotonin's involvement in many psychiatric disorders, which is mentioned in the following chapter.

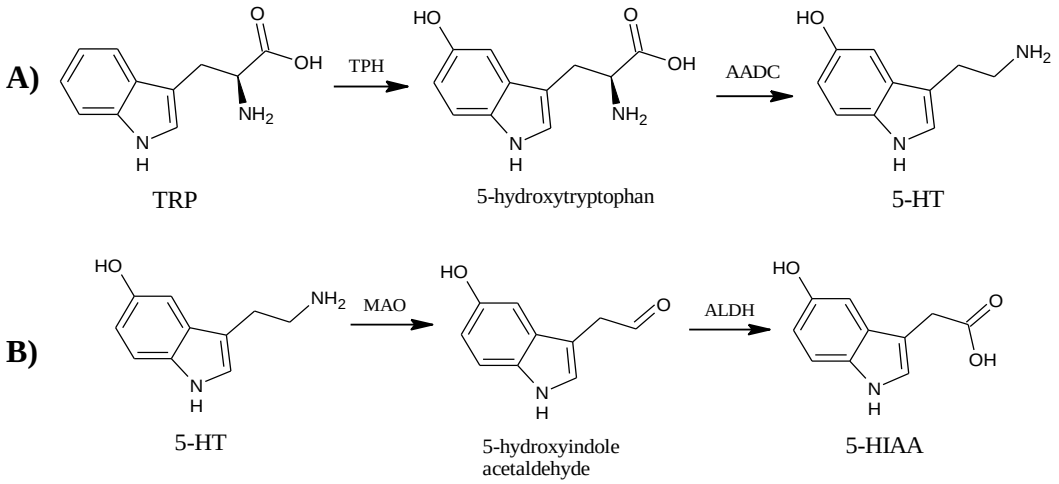

Fig. 3: *Metabolism of serotonin* ***A)*** *Serotonin synthesis; TRP is tryptophan, TPH tryptophan hydroxylase, AADC aromatic amino acid decarboxylase* ***B)*** *Serotonin degradation; 5-HIAA is 5-hydroxyindoleacetic acid, MAO monoamine oxidase, ALDH aldehyde dehydrogenase.*

2.1.4 Brain Diseases Associated with Abnormal Levels of Serotonin

Disruptions of serotoninergic neuronal system are correlated with diseases such are major depressive disorder, anorexia nervosa, and a group of anxiety disorders like panic disorder, obsessive-compulsive disorder, and social phobia.

As was mentioned in the chapter about dopamine related diseases, major depressive disorder is also influenced by serotonin. More specifically, by decreased 5-HT synthesis caused by lower amount of its precursor, decreased 5-HT release, reuptake or metabolism, or incorrect function of 5-HT receptors. This may cause fluctuations in appetite and sleeping patterns, mood, activity, or sexual behaviour, which are all signs of depression. Depression can be medicated by SSRIs (selective serotonin reuptake inhibitors) drugs that focus specifically on serotonin reuptake, or SNRIs (serotonin norepinephrine reuptake inhibitors) influencing serotonin and norepinephrine.[2,5]

Serotonin has a hypophagic effect (diminishes appetite), thereby inhibits feeding. It is an anorexigenic molecule; abnormal levels of serotonin are found in patients diagnosed with eating disorder anorexia nervosa (AN). AN is a lethal disorder strongly influenced by genetics. Patients suffering anorexia nervosa respond poorly to SSRI medication

due to their disrupted serotonin neurocircuitry – reduced serotonin release and increased 5-HT_{1A} receptor activity.[6]

There is a hypothesised connection between the serotoninergic neuronal system and a group of anxiety disorders (obsessive-compulsive disorder (OCD), social anxiety disorder, and panic disorder) mostly because of their positive response to SSRI medication. Serotonin's role in these illnesses is associated with distorted evaluation of social situations, anticipatory anxiety, fear, and panic attacks. Mechanisms of these complex emotions are tangled through many brain regions where 5-HT plays an important role.[7]

2.2 Methods Used for Detection of Neurotransmitters

It is important to have a reliable method of detection for neurotransmitters from biological samples (blood, urine, cerebrospinal fluid, or brain tissue). Physiological samples contain small amount of neurotransmitters, of the order of nanomoles.[32,33] That is why methods used for their detection must be very sensitive, and preferably without the need of any primal preconcentration. Two groups of methods are usually used for this purpose – liquid chromatography coupled with mass spectrometry (LC-MS) or electrochemical methods (cyclic voltammetry, CV).

Mass spectrometry (MS) itself is not sensitive enough, therefore it is often coupled with high performance liquid chromatography (HPLC). LC-MS technique has higher level of selectivity than electrochemical methods, but it requires sample preparation, which prolongs the analysis altogether. However, the limits of quantification are very low, up to the order of pg for dopamine[8].

Electrochemical methods exhibit lower limits of detection (pmol in brain tissue)[34] but are more susceptible to interferences. Therefore, physiological matrix presents a notable problem. Cyclic voltammetry is commonly used for neurotransmitters detection but is not very selective and is prone to sensing unwanted analytes. Probably the most common interferent is ascorbic acid (AA). This problem has recently been proposed solutions based on modifying measuring electrodes, e.g., using cavity carbon-nanopipette electrodes[34], or utilizing a composite p-Aln/Ms-atCNTCPE that enhances electro-chemical behaviour and shifts the peak of AA away from the detected analyte (often dopamine)[9].

Alternative method for neurotransmitters facile detection is surface enhanced Raman spectroscopy (SERS). Its advantages are low limits of detection, possible automatization

of the process, and no need for preconcentration or the use of inner standards. SERS was used in this work.

2.2.1 HPLC-MS

Mass spectrometry is an analytical technique that separates ions based on their weight/charge ratio. It is often used for detection of biological analytes, including neurotransmitters.

Both neurotransmitters dopamine and serotonin were analysed in the work of *Schnell et al.*[35] with LC-MS/MS. They tested the influence of lithium treatment on striatal dopamine and serotonin levels on 3 types of mice. For quantification, they used isotopically labelled internal standards. The results are shown in pM/mg of tissue in Fig. 4. Dopamine levels vary after lithium treatment in two (orange and blue columns) out of three (black columns) types of mice. There are no significant differences in serotonin levels between the mice type nor before and after lithium treatment.

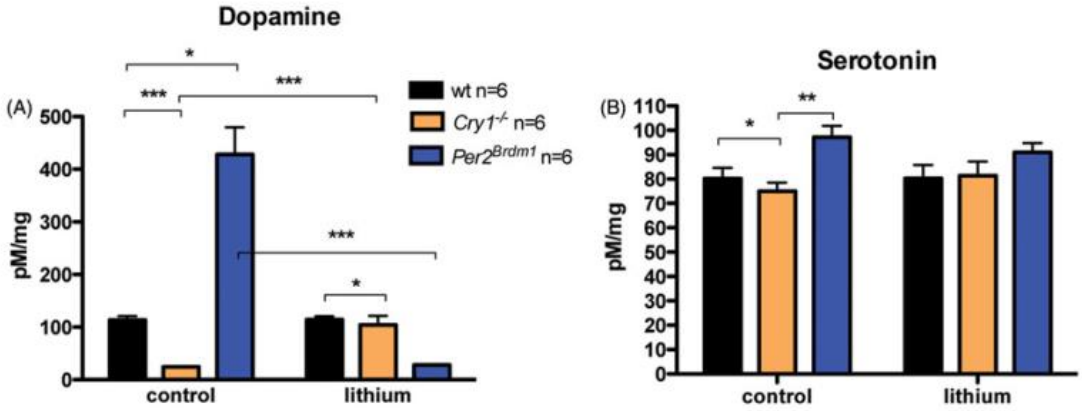

Fig. 4: *Striatal **A)** dopamine **B)** serotonin levels before and after lithium treatment on three types of mice. Black columns represent wild-type mice, orange columns Cryl knock-out mice, and blue columns Per2 mutant mice.*[35]

2.2.2 Cyclic Voltammetry

Another popular approach for detecting neurotransmitters is cyclic voltammetry.

To achieve greater sensitivity to specific analytes, measuring electrodes can be modified. For instance, *Urbanová et al.*[36] tried sensing dopamine (and NADH, ascorbic acid) with glassy carbon electrode (GCE) covered in fluorinated graphene with various levels of fluoride. The cyclic voltammograms for dopamine are shown in Fig. 5A (5 mM). The electrode covered with fluorographene with the least amount of fluorine ($CF_{0,084}$) shows best results. The overpotential needed for dopamine oxidation is the lowest here.

Based on further experiments, it is an adsorption-controlled process where π-π stacking interactions and H-bonding to fluorine play the biggest role (Fig. 5B shows dopamine configuration on $CF_{0,084}$), and it has the best sensitivity towards dopamine compared to other examined electrodes (bare GCE, graphene, and fluorographene covered GCE with higher fluorine concentrations). But the limit of detection in this work is only 0.57 μM.

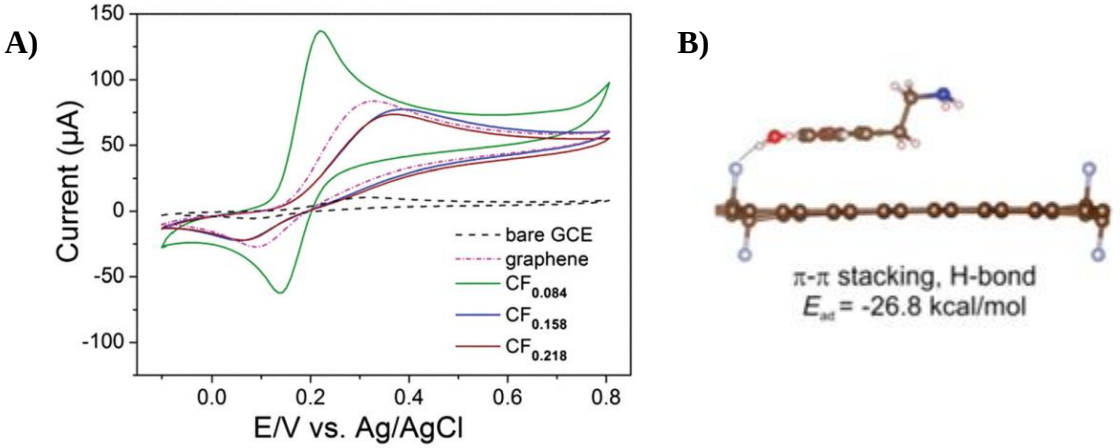

Fig. 5: A) *Cyclic voltammogram of dopamine solution (5 mM) measured by bare GCE (dashed black line), graphene (dashed-dotted purple line), and variously fluorinated graphene (green line stands for $CF_{0,084}$, blue line for $CF_{0,158}$, and red line for $CF_{0,218}$).* ***B)*** *Dopamine configuration on $CF_{0,084}$. Brown atoms are C, grey F, red O, beige H, and blue N. The calculated adsorption energy is -26.8 kcal.mol^{-1}.*[36]

In a more recent study, simultaneous analysis of four different analytes, including dopamine and serotonin, was achieved using a functionalized carbon paste electrode (CPE). It was modified with a composite composed of MoS_2/acid-treated multi-wall carbon nanotubes and covered with polymerized alanine (p-Aln/Ms-atCNTCPE). Such structure enhances electrochemical behaviour due to MoS_2 and its synergy with MWCNTs, and thanks to negative charges in poly-alanine layer enables shift of ascorbic acid's (AA) oxidation peak away from DA's peak to a more negative potential. The cyclic voltammogram of all four analytes can be seen in Fig. 6. Concentration of DA was 20 μM, of SE 18 μM, and of AA 400 μM. LOD for both neurotransmitters was in the order of μM.[9]

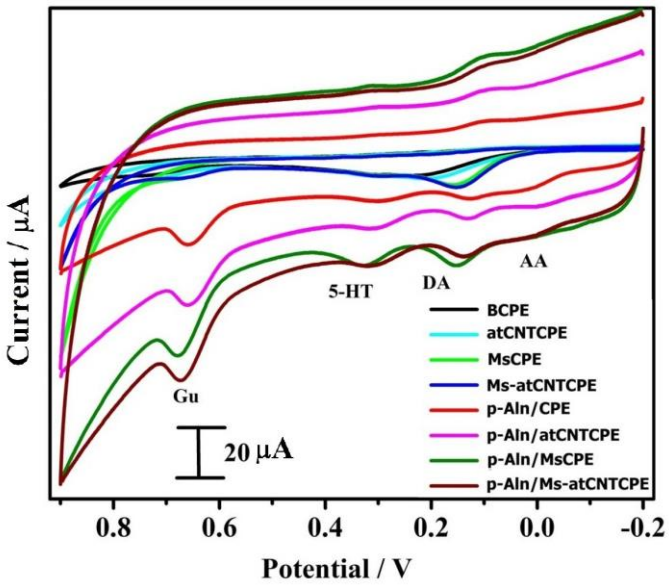

Fig. 6: *Cyclic voltammogram of a mixture of DA (20 μM), SE (18 μM), AA (400 μM), and guanine (Gu, 18 μM) in a PBS solution sensed by p-Aln/Ms-atCNTCPE (green line) and different electrodes. For more information, see Kumar et al.*[9]

2.2.3 The Basis of Surface Enhanced Raman Spectroscopy

Another very useful method for detection of various substances in low concentrations (up to single molecule detection)[37] is surface enhanced Raman spectroscopy (SERS).

Raman spectroscopy is an analytical technique using laser light of a specific wavelength (532 nm, 633 nm, 785 nm) to excite observed molecules to a virtual state. Later the inelastically scattered light is detected. This can either be the Stokes lines, if the molecule lowers its energy from the excited virtual state to a higher vibrational state than it occupied before the absorption while emitting a photon of appropriate wavelength, or the anti-Stokes lines, when the observed molecule originally had a higher vibrational state than the minimal one, but after emission it reaches the lowest vibrational state (see Fig. 7).

During Stokes scattering, the illuminated molecule is promoted to a higher energy level, and during anti-Stokes scattering, energy from the molecule's original higher vibrational level is transferred to the scattered photon. If the energy of adsorbed and emitted photon is the same, such process is called elastic Rayleigh scattering. This is the most common event – only one in 10^6 – 10^8 scattered photons is inelastically scattered, and therefore usable for Raman spectroscopy.[38]

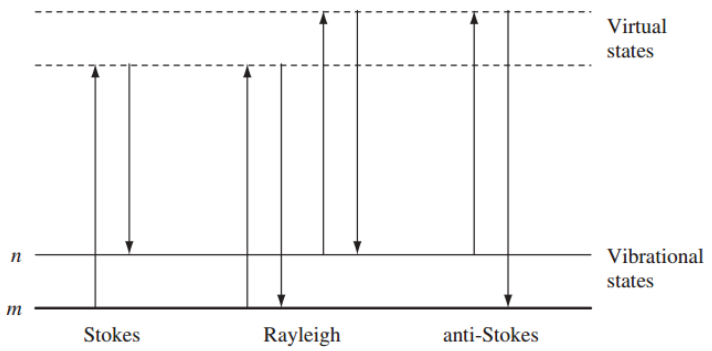

Fig. 7: *Diagram showing photon absorption (ν_{ab}) and emission (ν_{em}). If $\nu_{ab} = \nu_{em}$, it is Rayleigh elastic scattering, if $\nu_{ab} > \nu_{em}$, Stokes scattering, and if $\nu_{ab} < \nu_{em}$, anti-Stokes scaterring.*[38]

Most molecules occupy the lowest vibrational state at room temperature, as can be proved by the Boltzmann equation (Eq. 1), where N_n is the population of higher vibrational state n, N_m is the population of lower (or the lowest) vibrational state m, ΔE is the energy difference between starting and ending point of the molecule during photon absorption and emission, k_B is the Boltzmann constant and T is thermodynamic temperature.

$$\frac{N_n}{N_m} = e^{-\frac{\Delta E}{k_B T}} \qquad \textbf{Eq. 1}$$

Consequently, Stokes lines are much more prominent than anti-Stokes lines in the measured spectra.

Some molecules, especially biological ones, fluorescence. Fluorescence is a type of photoluminescence that occurs after the absorption of light, when the molecule is excited to a higher energy level, usually from S_0 to S_1 (ground state singlet to first excited state singlet). The excitation promotes the molecule to a higher vibrational state of singlet S_1, therefore the first process that occurs is internal conversion to S_1 ground state. From here, the molecule gets rid of its redundant energy by emitting a photon of appropriate wavelength. These photons represent fluorescence. It is best explained on the famous Jablonski diagram in Fig. 8.

This signal is seen in the same area as the Stokes lines, which makes the anti-Stokes lines more desirable to detect in Raman measurements for molecules that fluorescence.

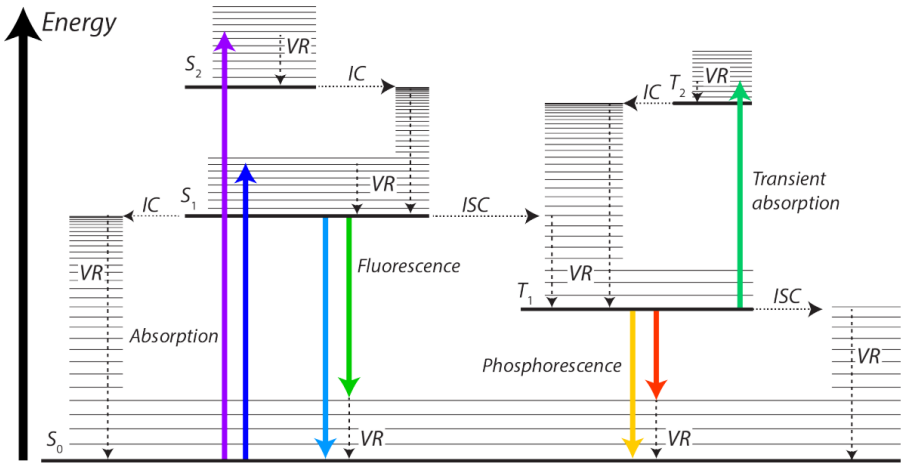

Fig. 8: *Jablonski diagram*[39] *– $S_{0/1/2}$ represents singlet at ground state (0), first and second excitation level (1 and 2), $T_{1/2}$ represents triplet at first and second excitation level, VR vibrational relaxation, IC internal conversion, and ISC inter system crossing*

Molecules that can be measured by Raman spectroscopy must change their polarizability upon interaction with light. This makes Raman spectroscopy supplemental to Infrared spectroscopy (IR) which detects the change of the dipole moment of a molecule. There is a rule for molecules with centre of symmetry that says if a specific vibration is active in Infrared spectroscopy, such vibration will not be seen through Raman spectroscopy, and the other way around. In conclusion, Raman spectroscopy is eligible for non-polar molecules, such are organic molecules, and Infrared spectroscopy for polar molecules, such are most inorganic ones.

This condition makes Raman spectroscopy desirable for many applications especially in life sciences. It allows measurements in water, a highly polar molecule, that gives minimal Raman signal.

To increase the signal of inelastically scattered photons, platforms from Ag, Au, or less often Cu are used, turning the method's name into **surface enhanced Raman spectroscopy (SERS)**. The platform can be metal nanoparticles (NPs) immobilized on solid surfaces or colloidal suspension of nanoparticles.

NPs size, proximity, and geometry play a very important role in the order of the enhancement. Solely appropriately small NPs (usually 5-100 nm) interact with the exciting light to induce Raman scattering. The limit for their smallest size emanates from quantum size effects (their size cannot be much smaller than the electronic mean free path of the conduction electrons of a metal), and the limit for their biggest size

is caused by the fact that incoming laser light would no longer excite dipolar plasmons in bulk metal but higher multipoles, which are non-radiative in Raman scattering.

Another condition for evoking Raman signal is NPs proximity. Only in aggregated form where particles are less than 1 nm apart there are so called hot spots. If an analyte is positioned in such hot spot, its Raman signal is enhanced by on average 10^6.[40]

An alternative way of achieving Raman enhancement other way than by aggregation is by changing NPs shape. The curvature of a NP influences the position of its surface plasmon resonance frequency and impacts its local electric field through 'lighting rod mechanism'. This mechanism defines the strongest electric field around the sharpest edges, which increases the amount and strength of hot spots around such NPs. That is why when comparing aggregated nanospheres, nanotriangles, and nanostars made of Au, their Raman efficacy will rise in this order, in accordance with their increasing number of sharp edges.[41]

There is a condition saying the exciting electric field vector must be polarized along the connecting line of the NPs, as shown on the bottom setting in Fig. 9A.[40] Only in this arrangement the dipoles enhance each other, therefore also amplify the signal of a molecule sitting in their interstice (hot spot). An experiment by *Jeong et al.*[42] shows this by measuring Raman spectra of Rhodamine 6G on silver nanowires aligned parallelly in two directions, using two different orientations of the electric vector. Hot spots also explain why isolated nanoparticles do not enhance Raman signal.

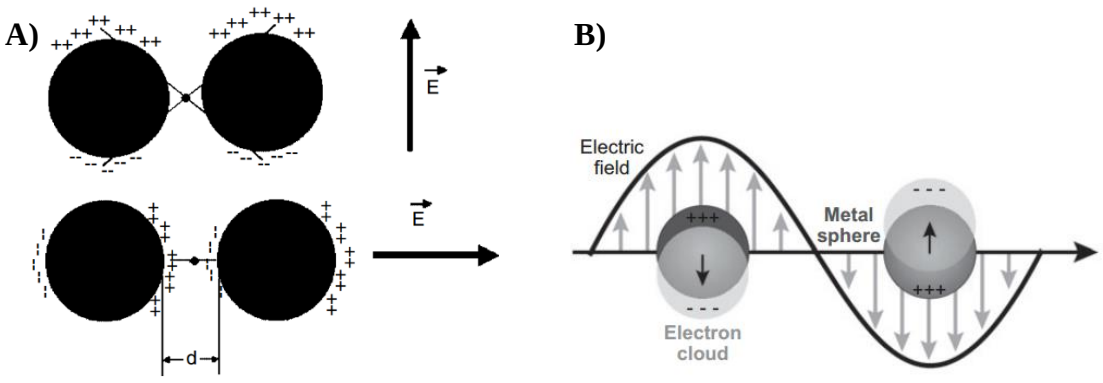

Fig. 9: A) *Orientation of the electric field vector perpendicular (top) to the connecting line of the NPs (black spheres) showing no enhancement for the analyte sitting in between them, and orientation coincident (bottom) with the connecting line of the NPs, showing great enhancement due to interaction of each NP with the incident beam and NPs oscillating dipoles together*[40]

B) *Localized surface plasmon resonance effect*[43]

NPs increase inelastic scattering of nearby molecules through surface plasmonic oscillation. This localized surface plasmon resonance (LSPR) occurs when oscillation of valence electrons is collective and in resonance with the incident radiation, as shown in Fig. 9B.[43] Such phenomenon is mostly explained by the **electromagnetic theory** (EM theory). It resolves the enhancement's dependence on the wavelength of the incident beam. This is due to NPs dielectric constant's dependence on the wavelength. For silver and gold NPs, it is wavelengths in the visible region that are in resonance with the metal's dielectric constant. The EM theory also defines the E^4 enhancement factor through a simplified equation (Eq. 2). Symbols used in this equation are: g is a value connected to dielectric constants as stated in Eq. 3 (ε_{in} is the dielectric constant of the metal NP, and ε_{out} is the dielectric constant of the external environment) and can be visualized as the averaged field enhancement over the NP's surface.[40,43]

$$|E|^4 = |g|^4 \qquad \textbf{Eq. 2}^{40}$$

$$g = \frac{\varepsilon_{in} - \varepsilon_{out}}{\varepsilon_{in} + 2\varepsilon_{out}} \qquad \textbf{Eq. 3}^{43}$$

These effects enhancing the Raman signal described by the electromagnetic enhancement theory are not dependent on the presence of an adsorbate. On the other hand, **chemical enhancement** relies on physical contact between the adsorbate and NPs. Its effect is through either charge transfer between the NPs and adsorbed molecule, or through resonant excitation of the adsorbate itself. The chemical enhancement is of a lower order then the electromagnetic enhancement, about 10^2-10^3.[40]

Any Raman active molecule positioned in a hotspot will emit high intensity signal. That is not advantageous in the presence of unwanted analytes that add background noise. One option for eliminating these interferences is to pre-treat the sample to get rid of unnecessary analytes, e.g., by membrane electrophoresis[44] or extraction techniques (e.g. borate plate for selective DA extraction from blood plasma[45]). However, such procedures may be time consuming. Another approach is to use labelled NPs. Labels can be organic molecules (iron nitriloacetic acid for the detection of DA[46]) or biomolecules (antibodies[47], aptamers[48]), covalently attached to NPs, that selectively bind the analyte. In other cases, mathematical analysis can be applied to the complex measured spectra. This method is non-disruptive to the sample, label-free, does not require any pre-treatment, and can interpret complex spectra. An example of mathematical analysis can be multivariate statistical method composed of principal component analysis (PCA) and least square discriminant analysis (LDA).[49] It was used together with partial least

squares regression (PLS) for diagnosing colorectal cancer based on SERS sensing of proteins albumin and globulin.[44]

2.2.3.1 SERS Sensing of Dopamine and Serotonin

Surface enhanced Raman spectroscopy was proved to give Raman signal of both dopamine and serotonin using various platforms. Both silver and gold nanoparticles, or silver-gold clusters were used. The platform can have different forms – from a simple colloid solution, through NPs immobilized on e.g., glass platform[14], some graphene derivative[12], or porous silicon[50], to a magnetic nanocomposite[46]. The overview of most works detecting dopamine and/or serotonin by SERS from 2014 till now (May 2021) are shown in Table 1.

Table 1: *Overview of most works detecting dopamine and/or serotonin by SERS from the year 2014 till May 2021 classified by used platform – Au colloid, immobilized AuNPs, Ag colloid, immobilized AgNPs, Ag+Au nanocomposite, or nanocomposite of magnetic NPs with AgNPs*

	Au colloid	Au immobilized	Ag colloid	Ag immobil.	Ag+Au	MNP @Ag
Dopamine	4[10,51–53]	11[12–14,54–61]	5[11,15,51,62,63]	5[33,50,64–66]	3[45,67,68]	1[46]
Serotonin	4[10,51,53,69]	7[12–14,55,59,69,70]	3[11,15,51]			

The main difference between Au and Ag NPs lies in AuNPs advantageous biocompatibility and stability in aqueous solutions and in AgNPs higher Raman signal enhancement.[45,67] These features can be connected, using a bimetallic platform – e.g., core-shell NPs (Ag-Au) were used for the detection of dopamine from aqueous solutions with various pH levels[67], Ag shell on Au nanorod dimers used for detection of dopamine enhanced the LSPR of AuNPs 6 times[68], or Ag layer on an amino terminated glass platform with bound AuNPs allowed forming higher amount of hot-spots between AuNPs through a hierarchical morphology for the detection of DA (LOD 10^{-11} M)[45].

Most researchers chose to use AuNPs in some form as a signal enhancing platform for both dopamine and serotonin. This may be attributed to the amines included in their structure that in their protonated, positively charged form interact with high affinity with the negative surface of AuNPs.[58] The dissociation constants were calculated and show that serotonin has significantly higher affinity towards AuNPs ($1.7 \cdot 10^{-10}$ M)

than dopamine ($5.7 \cdot 10^{-4}$ M), as it dispones of one additional nitrogen in its indole core. The experiments also propose a role of serotonin's cooperative effect. Such results indicate that dopamine and serotonin cannot be detected simultaneously with pure AuNP platform, as only serotonin would adsorb on the platform.[10,55]

Moody and Sharma (2018)[51] examined the best laser wavelength and nanoplatform to sense seven neurotransmitters, including dopamine and serotonin, in an aqueous solution. The best conditions for sensing dopamine in this work were achieved using excitation wavelength 785 nm with Au colloid, while for serotonin it was at 633 nm and Ag colloid. In each case, the limit of detection was 200 nM.

However, other works achieved even lower limits of detection, using altered NP platform and other experimental conditions. For example, employing a modified filter paper with immobilized AuNPs shaped as concave cubes, serotonin was detected at concentration 100 nM.[70]

Label-free detection of dopamine and serotonin with respective LOD 20 nM and 90 nM was achieved using AuNPs enclosed in PVP (polyvinylpyrrolidone).[10] In other work, the LOD was even lower, namely 0.001 nM, which was achieved through label-free detection in a dried drop composed of Ag colloid mixed with neurotransmitters, employing laser excitation wavelength 532 nm.[11]

Picomolar label-free detection of dopamine in aqueous solution at pH 8.5 was accomplished in the work by *Tezcan et al.*[58] by employing low-branched AuNPs aggregated on a glass platform.

For sub-picomolar dopamine detection, indirect methods have successfully been developed. *Jiang et al.*[64] measured Raman signal of ABTS (2,2'-azino-bis(3-ethylbenzthiazoline-6-sulfonic acid) diammonium salt), a compound that selectively oxidates in the presence of DA under specific conditions, on immobilized AgNPs platform. With this approach they achieved LOD for dopamine 0.32 pM. *Tang et al.*[68] achieved even lower LOD (0.006 pM) by employing Au nanorods functionalized with short complementary DNA strands (to form dimers) and covered with a Ag layer to further enhance the signal. They sensed DA indirectly by measuring the 1075 cm^{-1} peak of 4-aminothiophenol, a standard Raman probe. Or in a similar work, *Li et al.*[33] achieved dopamine's LOD 10 aM in PBS and 10 fM in serum by using an aptamer-modified probe that forms nanodimers.

Lee et al.[59] recently proposed a new technique called spread spectrum SERS (ss-SERS) that uses mathematical analysis to greatly enhance the signal to noise ratio of conventional

SERS. The trick of this method lies in exciting molecules with pulses of coded light and later reconstructing only the analyte's signal clear of all interference by applying peak autocorrelation and near-zero cross-correlation. For the detection of neurotransmitters, PCA was applied for the extraction of specific Raman peaks. With this novel approach, they achieved attomolar label-free detection of five neurotransmitters in a saline solution, including dopamine and serotonin.

Detection of DA and SE was also performed in a more complex matrix than deionized water, e.g. in artificial urine and artificial cerebrospinal fluid (aCSF), using a Au colloid to sense 50 μM concentration of these neurotransmitters.[51] Dopamine detection in nanomolar concentration was achieved from fetal bovine serum (FBS) by low-branched AuNPs immobilized on a glass platform.[58] A different work sensed dopamine at physiological concentration secreted from dopaminergic neurons immersed in saline physiological buffer[56], or DA released in-situ from dopaminergic neurons after being supplied with medications with a novel microfluidic biosensor[33].

DA was also sensed from blood plasma after its selective extraction with the use of a Au/Ag nanocluster[45], or from centrifuged serum with AgNPs adsorbed on $Ti_3C_2T_X$ nanosheet[65]. Quantitative determination of DA blood serum levels was determined by applying aptamer-modified SERS sensor[33].

Using a more complex signal enhancing platform made of AuNPs, DA antibodies, and barcode DNA, *Jeung et al.*[61] achieved reproducible detection of dopamine from midbrain, striatum, and plasma of mice at concentration $10^{-12} – 10^{-13}$ M.

Finally, in a very interesting work, serotonin was detected through a cat skull, using surface enhanced spatially offset Raman spectroscopy (SESORS). To mimic brain tissue underneath a skull, serotonin was embedded in agarose gel, which is a known imitator of brain tissue. AuNPs, excitation wavelength 785 nm, and principal component analysis were applied to sense and distinguish the signal of an analyte in low concentration from a sublayer. With this method, it was possible to identify serotonin in 100 μM concentration.[69] Later the research continued and both dopamine and serotonin (along with other neurotransmitters) were detected through a rat skull, this time achieving LOD 400 nM for SE and 1 μM LOD for DA.[53]

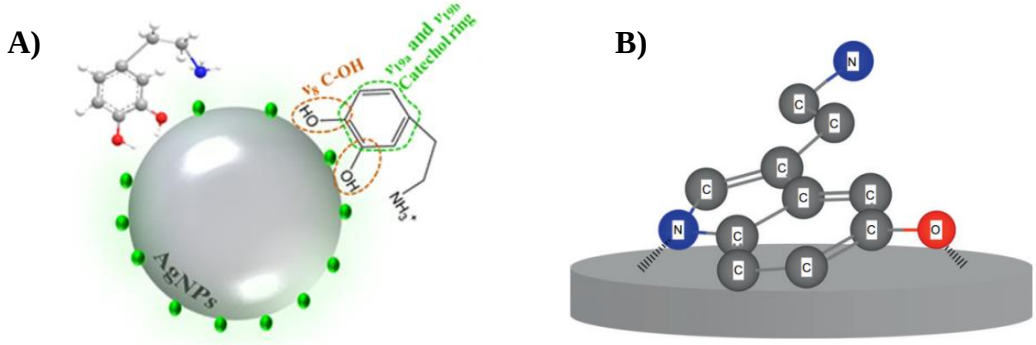

Fig. 10: A) *The most probable orientation of dopamine upon adsorption on AgNPs (grey aggregate) activated by NaCl (green dots). Hydroxyl groups of the catechol ring (red dots are oxygen) adsorb preferentially, with nitrogen atom (blue) having a secondary role.*[63] ***B)*** *Serotonin adsorption on Ag surface through indole nitrogen and hydroxyl oxygen at pH 11.*[71]

Dopamine adsorption on AgNPs was examined by *Figueiredo et al.*[63] in a theoretical study combined with laboratory experiments. Their results show a good match of experimental Raman spectra of dopamine with calculated Raman spectra for dopamine in a protonated form DA-NH_3^+. The scheme of beforementioned form of dopamine adsorbed on AgNPs activated by Cl^- ions is shown in Fig. 10A. Hydroxyl groups of the catechol ring of dopamine (red dots signifying oxygen) adsorb preferentially on AgNP, and nitrogen atom (blue) adsorb secondary.

For the case of serotonin adsorption on Ag surface, *Song et al.*[71] proposed adsorption through indole nitrogen and hydroxyl oxygen (Fig. 10B) at pH 11 ($c = 10^{-6}$ M).

2.2.3.2 Simultaneous Detection of Dopamine and Serotonin

Simultaneous analysis of dopamine and serotonin was only published four times so far.[12–15] In most articles, gold nanoparticles immobilized on an NH_2-functionalized glass platform[13,14] or covered with a graphene layer[12] were used as a Raman probe. In the last paper, AgNPs were used.[15] Table 2 compares consistent peaks from all these publications.

In one work, soda-lime glass was functionalized by two approaches – using magnetic stirrer or ultrasonic bath (novel). They achieved synthesis of highly monodispersed spherical AuNPs. They used laser excitation wavelength 532 nm and were able to distinguish both serotonin and dopamine in the presence of ascorbic acid (AA) at 10^{-7} M concentration. Peaks associated with serotonin are at 754, 833, 946, 1202, 1308,

1350, 1440, and 1547 cm^{-1}, and peaks associated with dopamine are at 1370, 1470, and 1622 cm^{-1}.[14]

Table 2: *Corresponding peaks of DA and SE from papers that simultaneously detect these neurotransmitters.* A *work used AuNPs on NH_2-functionalized soda-lime glass, laser 532 nm*[14]*;* B *work used AuNPs on NH_2-functionalized indium tin oxide glass, laser 633 nm*[13]*;* C *work used Au nanopyramids covered with a graphene layer, laser 633 nm*[12]*;* D *work used AgNPs colloidal suspension, laser 532 nm*[15].

	DA peaks (cm^{-1})			SE peaks (cm^{-1})						
A[14]	1370	1470	1622	754	833	946	1308	1350	1440	1547
B[13]	1370	1473	1624	751	828	943	1310		1440	1551
C[12]		1482								1547
D[15]					835	940	1308	1356	1435	1550

In another work, the functionalized glass was indium tin oxide (ITO) glass, onto which AuNPs were deposited electrochemically. They used laser excitation wavelength 632.8 nm and were also able to distinguish both serotonin and dopamine in the presence of ascorbic acid (AA, $c = 10^{-5}$ M) at 10^{-8} M concentration. Peaks associated with serotonin are at 751, 828, 943, 1310, 1440, and 1551 cm^{-1}, and peaks associated with dopamine are at 1142, 1370, 1473, and 1624 cm^{-1}.[13]

The respective spectra from beforementioned articles are shown in Fig. 11. Majority of the peaks assigned to dopamine and serotonin corresponds in both works, either with no or small deviation.

In the final paper using AuNPs that achieved simultaneous detection of dopamine and serotonin in an aqueous solution at concentration 10^{-10} M, Au nanopyramids covered with a graphene layer were used as a substrate. Main advantages of this substrate are: 1) possible mass production of highly homogenous nanopyramid AuNPs substrate and 2) mapping of the graphene superimposed surface prior to detecting analytes in low concentrations distinguishes exact locations of hotspots, ensuring sequential focus of the analyte.[12] This is possible because of the π-π interactions between the graphene layer and aromatic ring structures[72] in neurotransmitters – G-band of graphene with 1482 cm^{-1} peak of dopamine and 1547 cm^{-1} peak of serotonin[12] – chemically enhancing the SERS effect[73]. Here they used excitation wavelength 633 nm, and the resulting spectrum can be seen in Fig. 12.[12]

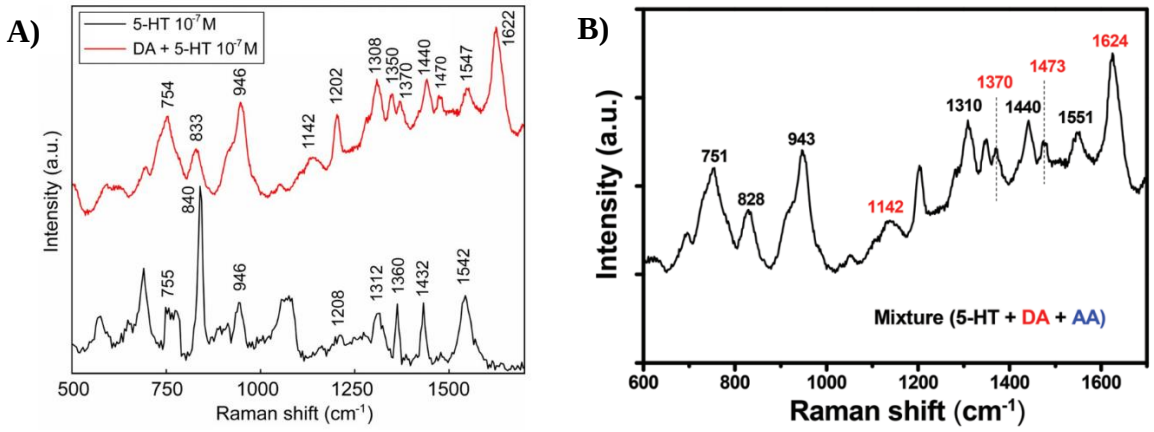

Fig. 11: *Spectra comparison of two studies detecting serotonin in the presence of dopamine and ascorbic acid (AA) in concentration* ***A)*** *10^{-7} M [14],* ***B)*** *10^{-8} M (AA 10^{-5} M)[13]. Matching serotonin peaks are 754 and 751 cm^{-1}, 833 and 828 cm^{-1}, 946 and 943 cm^{-1}, 1308 and 1310 cm^{-1}, 1440 and 1440 cm^{-1}, and 1547 and 1551 cm^{-1}, in A and B, respectively. Matching dopamine peaks are 1370 and 1370 cm^{-1}, 1470 and 1473 cm^{-1}, and 1622 and 1624 cm^{-1}, in A and B, respectively.*

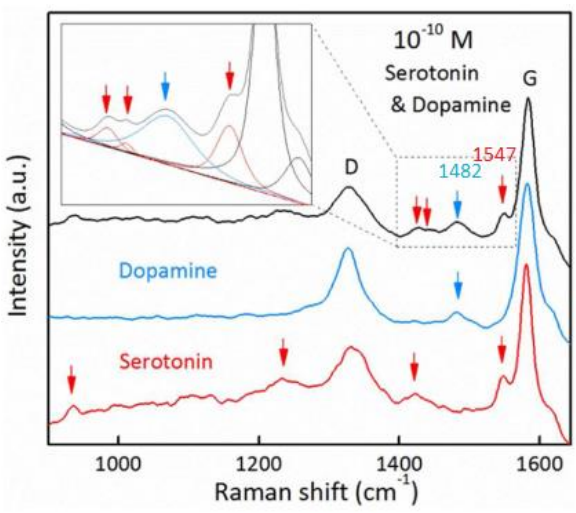

Fig. 12: *SERS signal of a mixture of dopamine and serotonin (10^{-10} M) aqueous solution sensed on Au nanopyramids superimposed with a graphene layer. The peak typical for dopamine is at 1482 cm^{-1}, peak typical for serotonin at 1547 cm^{-1},[12] which corresponds to peaks in previous studies in Fig. 11.*

In the remaining work[15], AgNPs and excitation wavelength 532 nm were used. Their results show how the Raman spectra is influenced by ranging ratios of dopamine and serotonin in a water solution (Fig. 13A) at concentration 10^{-9} M. They also present the possibility of a forming dopamine-serotonin composite, and support this with a theoretical study. The interaction of this composite is predicted to be

through a hydrogen bond between the oxygen atom on serotonin and -OH group in position 4 on dopamine (Fig. 13B). Their measured spectrum of 1:1 ratio of the neurotransmitters and corresponding simulated spectrum match well, positions of the most intense vibrational lines vary ±5 cm^{-1}. The probability of these neurotransmitters forming a composite is also supported by their neural proximity and similar function.

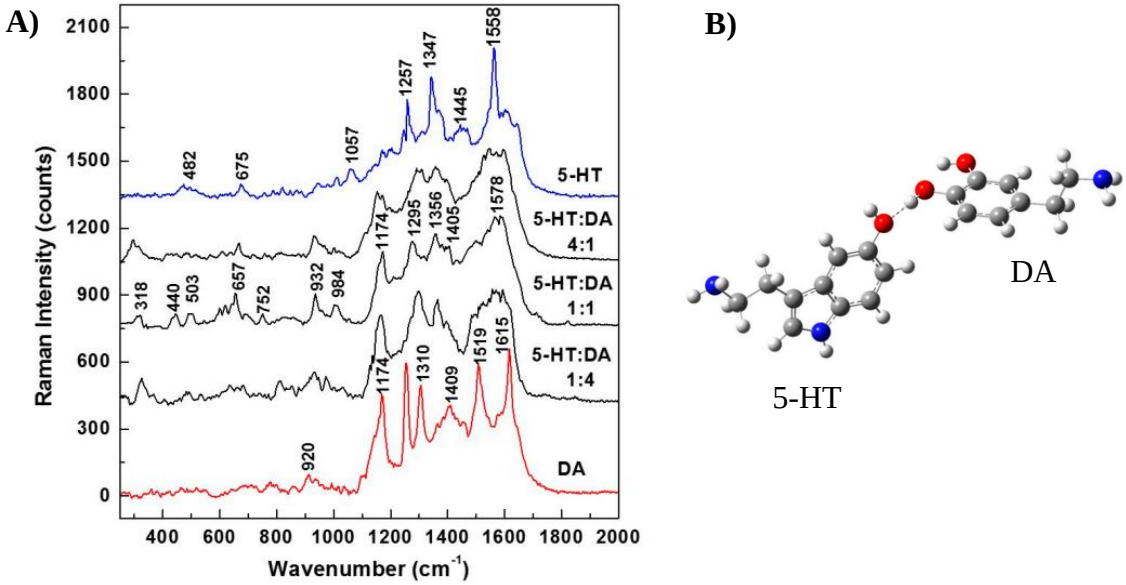

Fig. 13: A) *Measured spectra of mixtures of serotonin (5-HT) and dopamine (DA) (10^{-9} M) in ratios 4:1, 1:1, and 1:4. Spectra for pure serotonin (blue) and dopamine (red) are also shown.* ***B)*** *Simulated structure of the serotonin-dopamine composite held together by hydrogen bond*[15]

2.2.3.3 Magnetically Assisted Surface Enhanced Raman Spectroscopy

For easier separation of an analyte included in a complex matrix, a magnetic nanocomposite may be used. Such composite is assembled from a magnetic core (magnetite Fe_3O_4) and signal enhancing nanoparticles (AgNPs), glued together by appropriate linkers (polymers O-carboxymethyl chitosan or carboxymethyl cellulose CMC).[46,74,75] It can either be used in this bare form, or it can be further functionalized with targeting molecules (e.g. antibody[74], antidote[76], aptamer[48]). This allows specific separation of the target analyte from a complex matrix by simple application of external magnetic field and sample preconcentration before measurement, enabling analyte detection at low concentrations (10^{-9} M and lower).[46,74]

Magnetic composite can either be prepared in situ or bought, e.g., from Sigma-Aldrich (magnetic microparticles, carboxy functionalized). For laboratory preparation a protocol

by *Marková et al.*[77] is often used. Firstly, Fe_3O_4 nanoparticles are prepared by Massart coprecipitation method[78]. These NPs are then functionalized by adsorption of chitosan (or some other polymer) and reduction of silver ions and their immobilization.[77] By this process a nanocomposite with magnetite@chitosan@AgNPs structure is synthesised (Fig. 14).

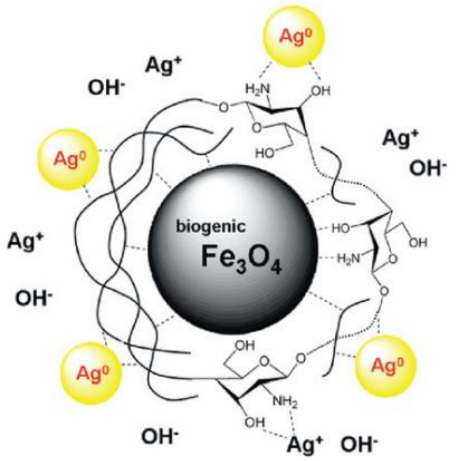

Fig. 14: *A schematic representation of synthesised nanocomposite magnetite@chitosan@AgNPs by Marková et al.*[77]

10 μL of such magnetic composite were mixed with 2 μL of a sample, stirred, and directly measured by Raman spectroscope in the work by *Ranc et al.*[46] They used magnetically assisted surface enhanced Raman spectroscopy (MA-SERS) to sense and quantify dopamine in artificial cerebrospinal fluid (aCSF) and mouse striatum. They used the previously mentioned nanocomposite, whose structure is schematically shown in Fig. 14, further functionalized by the addition of Fe-NTA (iron nitriloacetic acid), a dopamine selective compound. This nanocomposite was stable for 10 days and allowed amplification of dopamine signal to 10^{10}, allowing sensing dopamine in units of fM.

With this composite it was possible to detect dopamine in aCSF at concentration 50 fM (Fig. 15A) and in an extract from mouse striatum (Fig. 15B). For quantification of DA levels in striatum, they used the standard addition method. This approach is useful because it reduces matrix effects, hence improves accuracy.[74] Measured Raman spectra were smoothed by Savitsky-Golay algorithm and normalized.

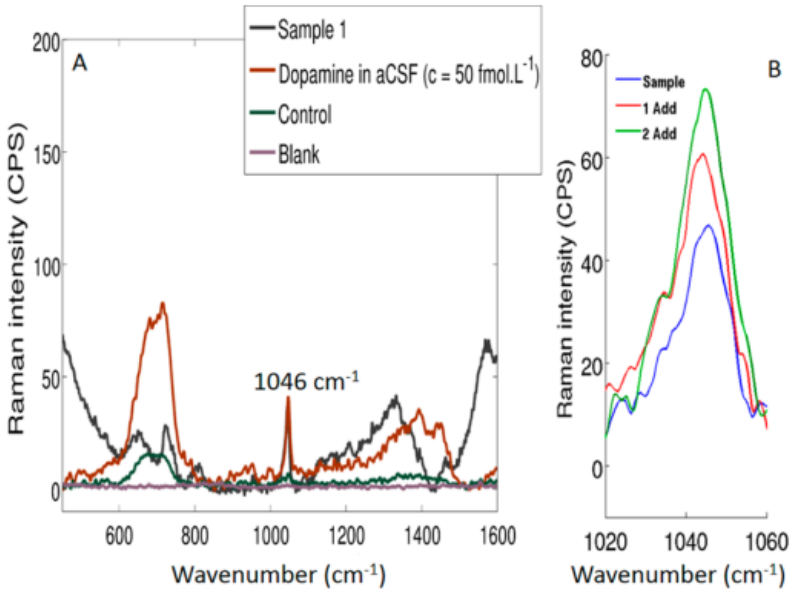

Fig. 15: A) *Measured Raman spectra of dopamine in artificial cerebrospinal fluid (dopamine concentration 50 fM, red line) and mouse striatum (clinical sample, black line). Control (magnetite@chitosan@AgNPs@Fe-NTA composite in aCSF, green line) and blank (magnetite@chitosan@AgNPs@Fe-NTA composite, lavender line) spectra are also shown.* ***B)*** *Two additions of 50 fM dopamine to striatum sample for quantification (standard addition method)*[46]

3 EXPERIMENTAL PART

3.1 Materials and Methods

3.1.1 Chemicals

Chemicals used for preparation of standard solutions of neurotransmitters are dopamine hydrochloride (certified reference material, TraceCERT®) and serotonin hydrochloride (≥98%) from Sigma-Aldrich.

For the preparation of artificial cerebrospinal fluid (aCSF), chemicals sodium chloride (≥99.8%), calcium chloride dihydrate (≥99%), magnesium sulphate (99%), and D-(+)-glucose (≥99.5%) from Sigma-Aldrich (St. Louis, USA), potassium chloride (≥99.5%), potassium dihydrogen phosphate (≥99.0%), and sucrose (99.8%) from Penta (Prague, Czech Republic), and sodium hydrogen carbonate (≥99.8%) from Lachema (Brno, Czech Republic) were used.

For extraction of neurotransmitters from brain tissue, a mixture of acetonitrile (≥99.5%) and acetic acid (99%) from Penta (Prague, Czech Republic) was used.

3.1.2 Methods and Software

For the analysis of neurotransmitters, DXR Raman microscope (Thermo Scientific, USA) was used with an excitation laser operating at 532 nm. Measurements were performed in full range from 58 – 3500 cm^{-1}. The spectra were typically acquired with a laser power 4 mW and exposure time 2 s. One experimental point was usually obtained by averaging of 32 microscans (less for neurotransmitters reference spectra in water and PBS, more for quantitative analysis). Fluorescence was corrected using a subtraction of polynomial fit, where n=3. Due to interference from cosmic rays, cosmic ray threshold was set to medium. All measurements were performed in a dried drop using 10 x objective lens.

For data processing, QtiPlot was used for figures of measured spectra. TQ Analyst software package (Omnic, version 8, Thermo Scientific, USA) was used for discriminant analysis performed on experiments distinguishing dopamine and serotonin in a mixture. The spectra were smoothed using Savitzky-Golay filter (data points 7, polynomial order 3), and the distinguishment was based on DA peak at 1485 cm^{-1} and SE peak at 1337 cm^{-1}.

3.2 Experiments

3.2.1 Preparation of Magnetic Nanocomposite

In this work, magnetically assisted surface enhanced Raman spectroscopy was applied for the detection of neurotransmitters dopamine and serotonin in different matrixes. The detection was enabled through a magnetic nanocomposite that is composed of a magnetic core and AgNPs. The magnetic core allows simple separation of analytes from a matrix, simple washing of the sample, and sample preconcentration in a drop before measurement. AgNPs greatly enhance the signal of detected molecules through LSPR. Above that, AgNPs immobilization on the magnetic composite guarantees high number of hot spots.

The magnetic nanocomposite was synthesised by Dr Medříková following modified protocol earlier described by *Balzarová et al.*[76] Magnetite NPs (MNPs) were prepared by Massart coprecipitation method of $FeCl_3 \cdot 6H_2O$ and $FeCl_2 \cdot 4H_2O$ at pH 11 (achieved by the addition of NaOH). The reaction took place at room temperature for one hour. Then MNPs were washed with ddH_2O three times. 200 mg of these MNPs were diluted in 19.5 mL of distilled water and acidified by adding 0.5 mL of 1M HCl.

Adsorption of carboxymethylcellulose (CMC) was achieved by adding 0.33 mL of CMC (1 g/30 mL of ddH_2O) to the MNPs. This mixture was stirred for 5 min on orbital shaker before being immersed in a water bath (80°C) for one hour.

After the mixture reached ambient temperature, 25 mg of silver ions were added in the form of $AgNO_3$, along with 0.5 mL of 10M NaOH. The reduction of Ag^+ took place in an 80°C water bath for 20 min. After reaching ambient temperature, the synthesised magnetic composite was washed three times. Its structure can be described with the following abbreviation MNPs@CMC@AgNPs.

3.2.2 Optimization of the Method MA-SERS

The goal of this work was to find out whether it is possible to detect dopamine and serotonin in a label-free manner with a magnetic nanocomposite. Their detection was performed in different matrixes varying from simple detection in an aqueous solution (distilled water), through detection in PBS solution, and artificial cerebrospinal fluid (aCSF), to detection in an extract from mouse brain tissue – striatum. It was also tested to see if simultaneous analysis of both neurotransmitters in ranging ratio was possible in PBS and aCSF solutions.

First it was important to optimize variables to obtain clear spectra of both neurotransmitters, preferably using the same experimental conditions. This consisted of sensing DA and SE dissolved in different solutions with the magnetic nanocomposite and optimizing Raman settings such are excitation laser wavelength, laser power, and number of exposures. Concentrations of DA and SE in these experiments were 10^{-3} M. Laser excitation wavelength 532 nm was chosen based on previous work by *Ranc et al.*[46] sensing DA with nearly identical composite.

During preliminary experiments, DA and SE were detected in an aqueous solution with the intention to identify their specific peaks with no matrix interference. Because DA is unstable in water[20], the same experiments were later performed using a PBS (phosphate-buffered saline) solution. For these experiments, 50 μL of diluted magnetic nanocomposite (50 μL + 950 μL of distilled water) were mixed with 10 μL of a neurotransmitter's solution (10^{-3} M) and stirred for 20 s in the case of aqueous solutions or 30 min in the case of PBS solutions. Later, samples were left for 30 mins to reach ambient temperature. Then the bonded analyte (DA or SE) was separated from the supernatant using magnetic decantation, washed 3 times with distilled water, and subsequently redispersed in 10 μL of distilled water. 2 μL of this final dispersion were dropped on a CaF_2 glass platform, magnetically gathered at a side of the drop, left to dry, and measured. This process can be found in appendices Fig. A7. All measurements were performed in a dried drop because it achieved higher signal than measurements from a liquid.

Raman conditions were tuned to achieve the best signal for each spectrum, which was laser power 4 mW in all cases, and varying number of exposures: 8 exposures for DA in PBS, 16 exposures for DA and SE in water, and 32 for SE in PBS.

As it was challenging to sense serotonin in PBS with somewhat distinctive peaks, more analyte (20 μL) was added to the magnetic composite.

This higher ratio (50 μL of magnetic composite mixed with 20 μL of the sample solution) was kept constant for experiments detecting DA and SE from artificial cerebrospinal fluid (aCSF). aCSF is a pure aqueous solution composed of salts and sugars in different concentrations, namely 2.5 mM potassium chloride, 2.5 mM calcium chloride, 124 mM sodium chloride, 2 mM magnesium sulphate, 26 mM sodium hydrogen carbonate, 1.25 mM potassium dihydrogen phosphate, 10 mM glucose, and 4 mM sucrose.[79] aCSF mimics biological environment, neurotransmitters natural occurrence,

and contains more interfering agents than PBS. However, dopamine oxidizes swiftly in this artificial CSF (unusable the next day), as is implied by the change of the colour of the solution from pure to grey (shown in appendices Fig. A6). Therefore, DA samples must always be measured on the day of preparation.

As prepared aCSF mixture was stirred through the night in a fridge for better quality of adsorption. Later, the same procedure was used, briefly the solutions were left to reach ambient temperature, washed 3 times, and redispersed in 10 μL of distilled water. 2 μL were then dropped on a glass platform, magnetically gathered at a side, left to dry, and measured. Neurotransmitter's detection in aCSF was performed by applying laser power 4 mW and 32 exposures.

In the attempt to get clearer spectrum of serotonin, laser excitation wavelength 780 nm was tested. Although dopamine gave strong and clear signal with this laser across wide range of tested laser power (0.9 – 20 mW), it was not possible to sense serotonin with any of this set-up. Therefore, laser excitation wavelength 532 nm kept being used in all experiments.

Naturally, spectra of blanks were measured before each experimental set with the same conditions later applied to samples. Types of blanks measured in this work are CaF_2 glass platform (Fig. A5), dried magnetic nanocomposite (MNPs), dried MNPs incubated with PBS solution, and dried MNPs incubated with aCSF.

3.2.3 Simultaneous Detection of DA and SE in PBS and aCSF

For identification of selective peaks for dopamine and serotonin in one sample, respective mixtures were prepared. The ratios of DA:SE were as follows: 1:1, 1:5, 5:1, 1:10, and 10:1, to determine the method sensitivity for each neurotransmitter in abundance (up to 10fold) of the other. The mixtures were prepared at first in PBS, a less complex matrix, and later in artificial cerebrospinal fluid, that contains more interferences, including saccharides.

Firstly, smaller set of experiments was performed to optimize the ratio of mixed components – magnetic nanocomposite and a sample. Three options were tested – 50 μL of the composite mixed with 10, 20, or 30 μL of a sample. Such samples were later measured under the same conditions, which is 4 mW and 32 exposures, to evaluate the best volumetric ratio. 20 μL were deemed the best.

These samples, dissolved in PBS, were stirred for 30 min, whereas samples in aCSF were stirred throughout the night in a fridge, in accordance with previous experiments.

Later, the same process as described above was applied. The spectra were obtained using laser power 4 mW and 32 exposures.

For data processing, a type of multivariate statistical analysis was performed, specifically discriminant analysis (TQ Analyst). Gathered spectra were first smoothed using the Savitsky-Golay algorithm (data points 7, polynomial order 3). This allowed reliable differentiation of both neurotransmitters in PBS and aCSF in all tested ranges.

3.2.4 Limit of Detection in aCSF with Magnetic Nanocomposite

For determining the limit of detection for both neurotransmitters, a 6-point calibration curve was assembled. The range used in these experiments was determined from previous measurements of different concentration orders – from 0.1 mM to 1 mM with 4 points in between (0.2 mM, 0.4 mM, 0.6 mM, and 0.8 mM).

These samples were mixed with 50 μL of the nanocomposite. For DA it was sufficient to add only 20 μL of the sample, whereas for SE it was 50 μL. Samples were stirred throughout the night in a fridge, washed three times with distilled water, and finally measured on the edge of a dried drop where the magnetic composite was gathered.

The applied laser power also differed for dopamine and serotonin due to serotonin's peaks low quality. 4 mW and 64 exposures were used when collecting DA spectra, and 1 mW and 128 exposures when collecting SE spectra. Gathered data were then processed to obtain linear calibration equations with respective R^2 values and limits of detection (LOD).

3.2.5 Measurements in Mouse Brain Tissue (Striatum)

Black mouse striatum was kindly supplied by the Faculty of Medicine, Palacký University, Olomouc. Animals were bred under constant humidity and temperature and had free access to food and water. 4-6 weeks old male mice were sacrificed, their brains dissected, and striatum separated. Samples were kept at -80°C covered in tin foil until measurements.

For the analysis, protocol by *Ranc et al.*[46] was applied. 1 mg of striatum was inserted into 10 μL of acetonitrile/acetic acid solution (0.98/0.02, v/v) for neurotransmitters extraction. This dispersion was then covered with a tin foil and sonicated for 15 min at room temperature. Later, 2 μL of extracted sample were added to 10 μL of the magnetic nanocomposite. As prepared samples were left to incubate during the night in a fridge under constant stirring.

The next day, the samples were washed, redispersed in 10 μL of distilled water, and measured. Spectra were again collected from a dried drop. The method was further tuned to achieve distinguishable peaks of DA and SE by changing laser powers and number of exposures. The clearest spectra were achieved when applying laser power 1 mW and 128 exposures.

4 RESULTS AND DISCUSSION

4.1 X-ray Powder Diffraction of the Magnetic Nanocomposite

The structure of synthesised magnetic nanocomposite, formally described as MNPs@CMC@AgNPs, was examined with X-ray powder diffraction. Measured spectrum with fitted peaks is shown in Fig. 16.

Majority of the composite, 82.7 %, was attributed to magnetic iron oxides magnetite Fe_3O_4 and maghemite γ-Fe_2O_3. The mean size of their coherent domains was 11 nm. The presence of maghemite was caused by heating during MNPs synthesis, which led to partial oxidation of magnetite to maghemite. Considering both iron oxides are magnetic, this was not a problematic finding, and no further analysis was performed to determine their ratio.

8.2 % of the composite was attributed to AgNPs with mean size of coherent domains 14 nm. Apart from these expected phases, $FeAgO_2$ was detected at 9.2 % of the magnetic nanocomposite. This phase results from direct interaction of silver with the magnetic nanoparticles. Its mean size of coherent domains was 16 nm.

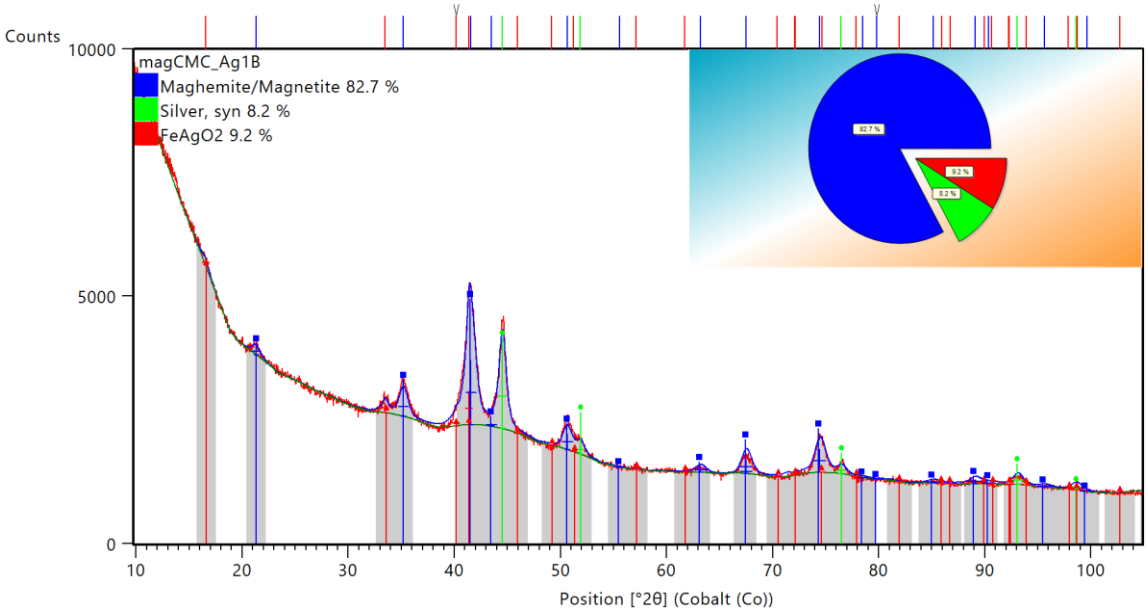

***Fig. 16**: Diffractogram of the magnetic nanocomposite with assigned peaks to the magnetic phase magnetite or maghemite (blue), AgNPs (green), and $FeAgO_2$ (red). The percentage of assigned phases are 82.7 % for magnetite and maghemite, 8.2 % of AgNPs, and 9.2 % of $FeAgO_2$. The mean size of respective coherent domains are 11 nm, 14 nm, and 16 nm.*

4.2 MA-SERS Detection of Dopamine and Serotonin

The best conditions for sensing both dopamine and serotonin with magnetic nanocomposite were achieved when laser excitation wavelength 532 nm was used with laser power 4 mW. Lower laser power gave lower signal and did not reveal enough detail in spectra, and higher laser power damaged the sample.

Spectra of dopamine and serotonin (10^{-3} M) in distilled water (black), PBS solution (pink), and artificial cerebrospinal fluid (aCSF) (blue) are shown in Fig. 17 and 19. Data reproducibility for aCSF solutions can be found in appendices, Fig. A1 and A2.

The intensity of dopamine is higher than the intensity of serotonin in all cases because of its higher affinity towards the composite. It is the same composite that was used in the work by *Ranc et al.*[46], that was specifically designed for sensing dopamine, but without Fe-NTA molecule.

The intensity of both neurotransmitters is the lowest for their aqueous solutions. For dopamine, intensity rises with more complex matrix – aqueous solution < PBS solution < aCSF solution. In this same order, the solutions better resemble neurotransmitters natural occurrence. For serotonin, spectra in PBS have the highest intensity. These results signify DA and SE higher stability in such conditions. However, samples in aCSF were incubated noticeably longer than samples in PBS, which in turn were incubated longer than samples in distilled water.

What is more important to mention about the spectra is that less details are noticeable in a more complex matrix. Especially spectra of DA and SE dissolved in aCSF show significantly less defined peaks than respective spectra of DA and SE in water or PBS. However, there are always some peaks specific for the neurotransmitter.

The most noticeable peak for dopamine is at 1485 cm^{-1}. It belongs catechol ring breathing. Other specific DA peaks are located at 1271 cm^{-1} (catechol C-O stretching), 1327 cm^{-1} (C-O stretching), and 1409 cm^{-1} (C-H wagging and N-H twisting).[11,58,59] The assigned DA peaks are shown in a close-up of the dopamine PBS solution spectra in Fig. 18.

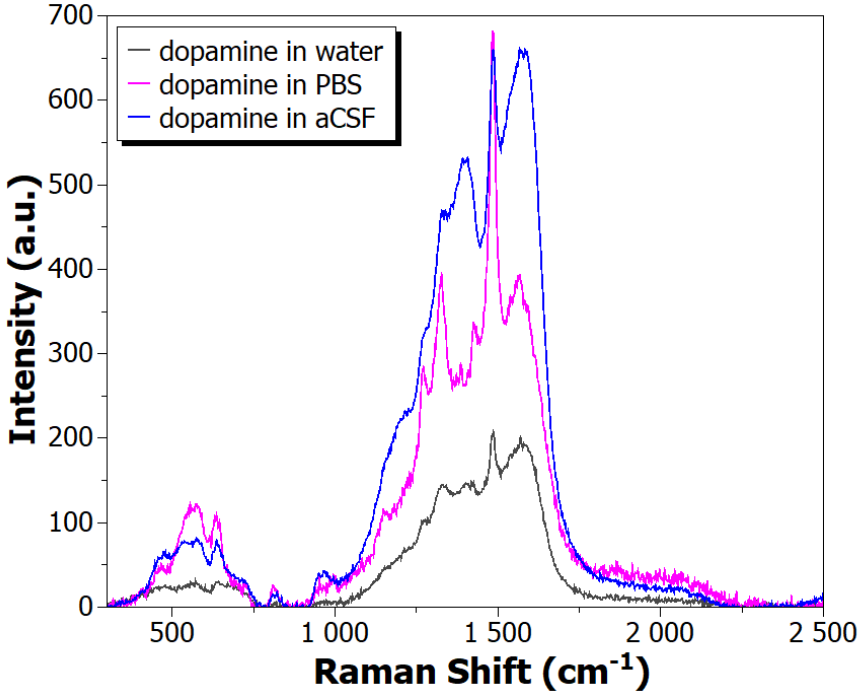

Fig. 17: *MA-SERS spectra of dopamine solutions (10^{-3} M) in distilled water (black), PBS solution (pink), and artificial cerebrospinal fluid (blue). Dopamine's characteristic peaks are visible from 1261 – 1588 cm^{-1}, with the most prominent one located at 1485 cm^{-1}. The peaks in the range 668 – 711 cm^{-1} belong to the signal enhancing nanocomposite. The spectra were obtained with laser excitation wavelength 532 nm and laser power 4 mW.*

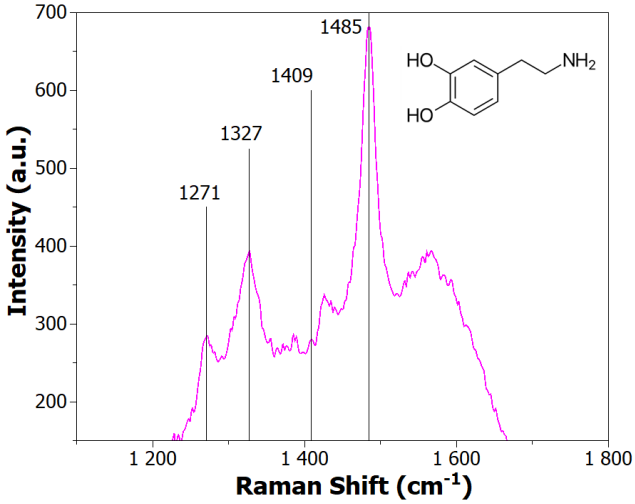

Fig. 18: *A close-up of assigned dopamine peaks at 1271 cm^{-1} (catechol C-O stretching), 1327 cm^{-1} (C-O stretching), 1409 cm^{-1} (C-H wagging and N-H twisting), and 1485 cm^{-1} (catechol ring breathing)*[11,58,59] *from dopamine spectra in PBS solution. The spectrum was obtained with laser excitation wavelength 532 nm, laser power 4 mW, and 8 exposures.*

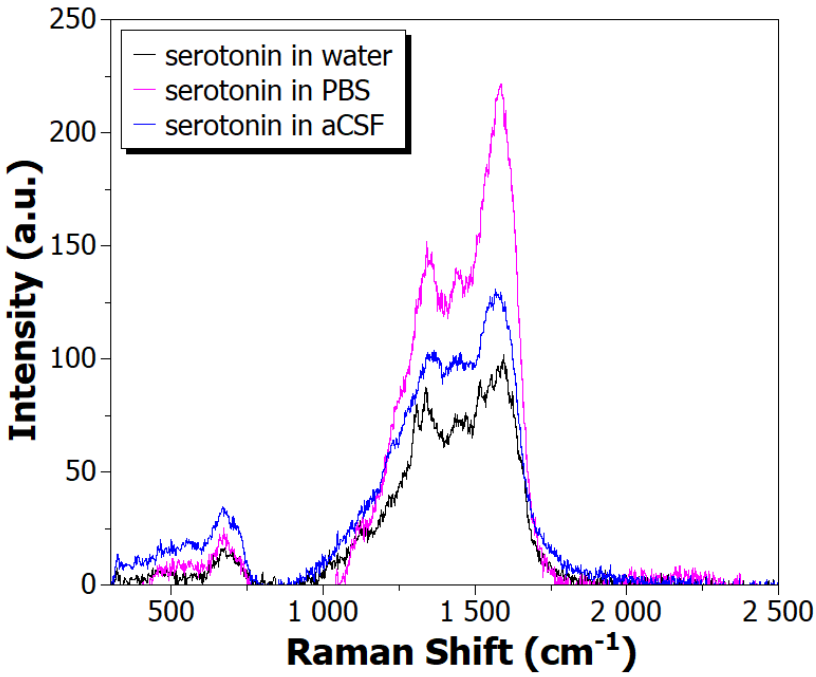

***Fig. 19**: MA-SERS spectra of serotonin solutions (10^{-3} M) in in distilled water (black), PBS buffer solution (pink), and artificial cerebrospinal fluid (blue). Serotonin's characteristic peaks are visible from 1306 – 1623 cm^{-1}. The peaks in the range 668 – 711 cm^{-1} belong to the signal enhancing nanocomposite. Spectra were obtained with 532 nm excitation wavelength, laser power 4 mW.*

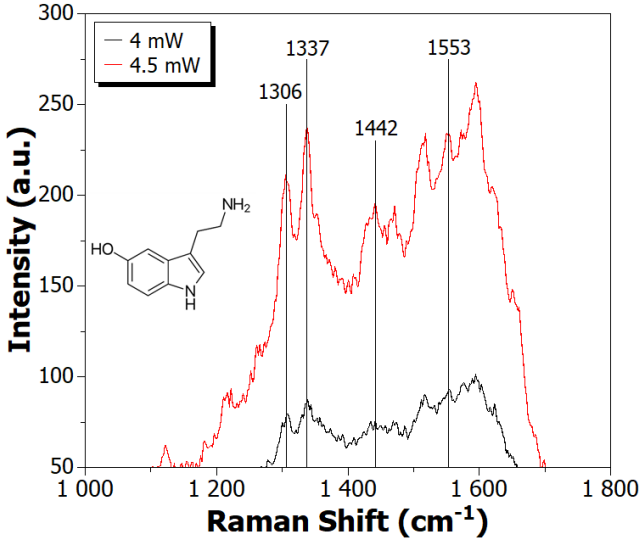

***Fig. 20:** A close-up of assigned serotonin peaks at 1306, 1337, 1442, and 1553 cm^{-1}, which all belong to in-phase breathing and stretching of the indole ring,[11,80] from serotonin spectra in distilled water. Spectra were obtained with 532 nm excitation wavelength, laser power 4 mW (black) or 4.5 mW (red). The figure proves reliability of serotonin identification at 4 mW, where peaks are less resolved. One spectrum was obtained by averaging 16 microscans.*

Serotonin does not have one nicely defined peak as dopamine, but it has at least four peaks proved by literature that belong to serotonin. Those occupy positions at 1306, 1337, 1442, and 1553 cm^{-1} , and are all classified as in-phase breathing and stretching of the indole ring that makes serotonin's core.[11,80] These peaks are more defined when higher laser power is used (4.5 mW), but can still be found in spectra measured at 4 mW, as can be seen in Fig. 20. Both spectra presented here are spectra of serotonin in distilled water.

At first glance, there seems to be some interference causing D and G bands-like distortions of both DA and SE spectra. It was suspected it could originate from some impurity of the composite or from adsorbed glucose or sucrose that are present in aCSF. However, this trend does not show in blank samples of the nanocomposite itself or nanocomposite incubated with PBS or aCSF solutions (Fig. 21). Moreover, a similar trend of two broader bands can be found for both dopamine[56,58] and serotonin[11,55,71] spectra from literature. Nevertheless, the spectra of blanks show that peaks in the range 668 – 711 cm^{-1} belong to the composite.

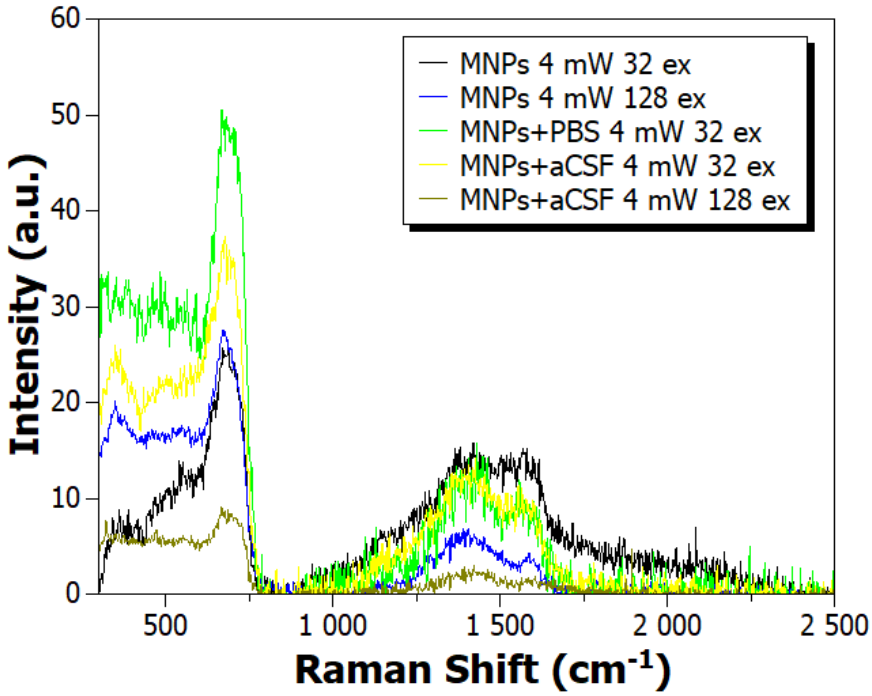

Fig. 21: *Spectra of blanks – sole magnetic nanocomposite (MNPs) measured at 4 mW with 32 exposures (black), sole MNPs measured at 4 mW with 128 exposures (blue), MNPs incubated with PBS measured at 4 mW with 32 exposures (bright green), MNPs incubated with aCSF measured at 4 mW with 32 exposures (yellow), and MNPs incubated with aCSF measured at 4 mW with 128 exposures (dark green).*

Another theory was that the broad bands come from partially burned samples. For this reason, laser with longer wavelength, 780 nm, was tested. Although dopamine gave strong and clear signal with this laser across wide range of tested laser power (0.9 – 20 mW), as can be seen in Fig. 22, it was not possible to detect serotonin with any of this set-up. Therefore, laser excitation wavelength 532 nm kept being used in all experiments. Afterall, those bands do not melt neurotransmitters peaks together even at long expositions (128, results are shown in the following chapter).

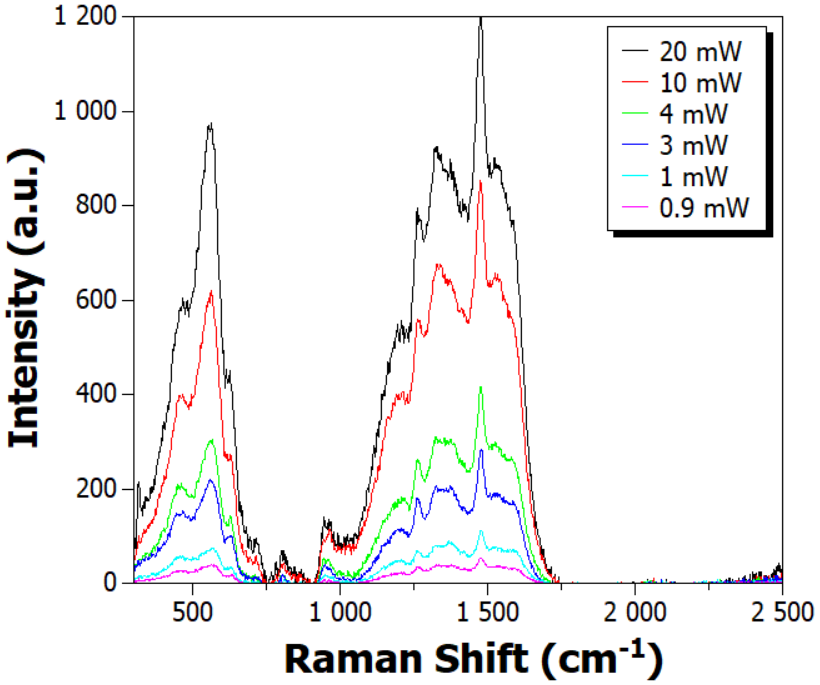

Fig. 22: *MA-SERS spectra of dopamine solutions (10^{-3} M) in aCSF measured with 780 nm laser with varying laser power – 20 mW (black), 10 mW (red), 4 mW (green), 3 mW (dark blue), 1 mW (turquoise), and 0.9 mW (pink). Dopamine's characteristic peaks are visible in two regions, from 1261 – 1588 cm^{-1}, with the most prominent one located at 1485 cm^{-1}, and from 444 – 624 cm^{-1}. The low peaks in the range 668 – 711 cm^{-1} belong to the signal enhancing nanocomposite.*

4.3 Simultaneous MA-SERS detection of DA and SE in PBS and aCSF

Another set of experiments focuses on whether it is possible to distinguish DA and SE in a mixture, even if there is a surplus one of the neurotransmitters. For this purpose, five mixtures of dopamine and serotonin in ratios 1:1, 1:5, 5:1, 1:10, and 10:1 were measured. The experiments were performed using PBS buffer and aCSF as a matrix.

Firstly, the ratio of MNPs with the analyte in PBS was tuned to achieve best resolution of the peaks. 50 μL of MNPs were mixed with either 10, 20, or 30 μL of the analyte. All such neurotransmitters' mixtures were measured under the same Raman conditions and compared. Because serotonin gives lower signal, the decision was made based on the spectra containing abundance of serotonin – 1:10 spectra. From the results it was clear that adding 20 μL of the sample is the most adequate amount (Fig. 23).

Fig. 24 shows measured spectra of mixtures in PBS and aCSF, respectively. In accordance with previous results, respective spectra in aCSF have higher intensity than those in PBS. Because dopamine has higher affinity towards the magnetic nanocomposite, spectra containing 10fold of DA compared to SE have the highest intensity, followed by 5fold of DA, and equal amounts of both neurotransmitters. There is little difference in the intensity of spectra of 5fold and 10fold of serotonin, owing to lower affinity of SE, that does not oversaturate the nanocomposite when higher amount of SE is used. There are again less details noticeable in aCSF spectra. Data reproducibility for mixtures in PBS and aCSF can be found in appendices, Fig. A3 and A4.

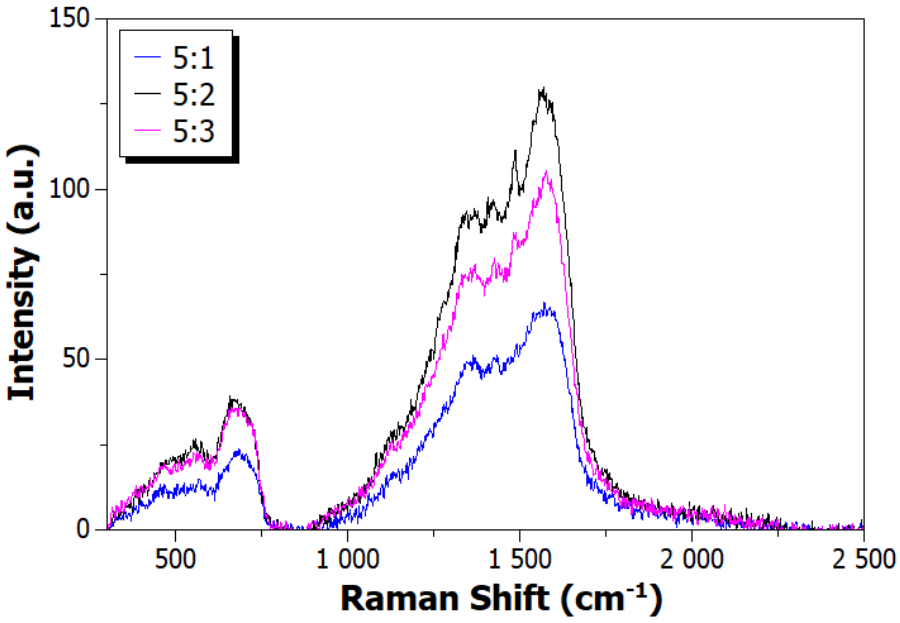

Fig. 23: *MA-SERS spectra of dopamine:serotonin mixture 1:10 in PBS in three volumetric ratios with the magnetic nanocomposite – 5:1 MNP:analyte (blue), 5:2 (black), and 5:3 (pink). All spectra were obtained with 532 nm excitation wavelength, laser power 4 mW, 32 exposures.*

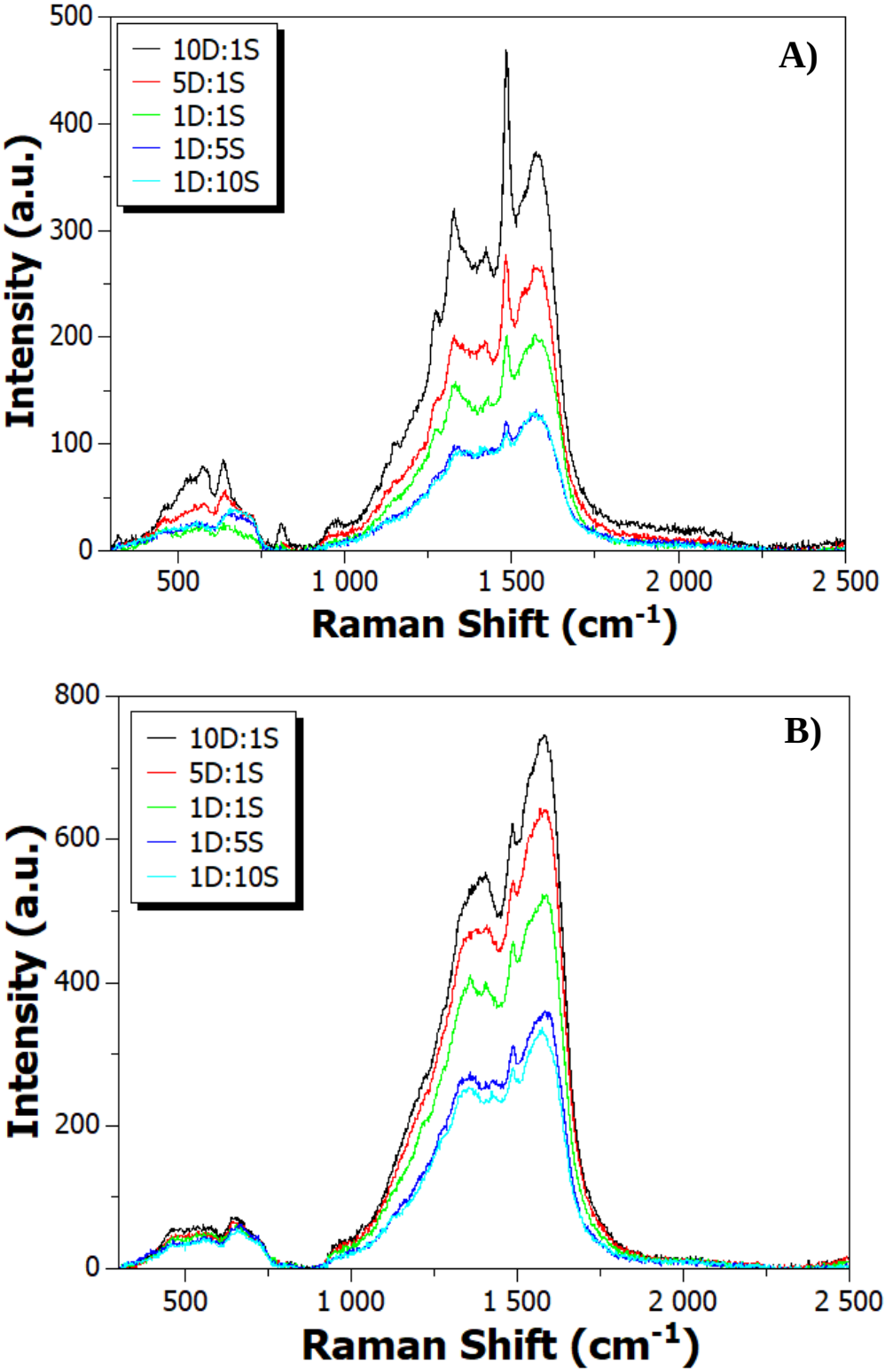

Fig. 24: *MA-SERS spectra of mixtures of dopamine and serotonin in ratios 10:1 (black line), 5:1 (red line), 1:1 (green line), 1:5 (blue line), and 1:10 (turquoise line) in* ***A)*** *PBS solution and* ***B)*** *artificial cerebrospinal fluid. The volumetric ratio of MNPs and the sample was 5:2 based on previous experiments. All spectra were obtained with 532 nm excitation wavelength, laser power 4 mW, and 32 exposures.*

Both neurotransmitters were successfully identified in measured spectra through discriminant analysis (TQ Analyst). The dataset of mixtures in aCSF required higher number of spectra (Fig. 25B) than in PBS (Fig. 25A) due to less clear peaks. Samples with abundance of serotonin were correctly assigned to SE (upper left corner, blue squares) and samples with abundance of dopamine to DA (bottom right corner, red triangles).

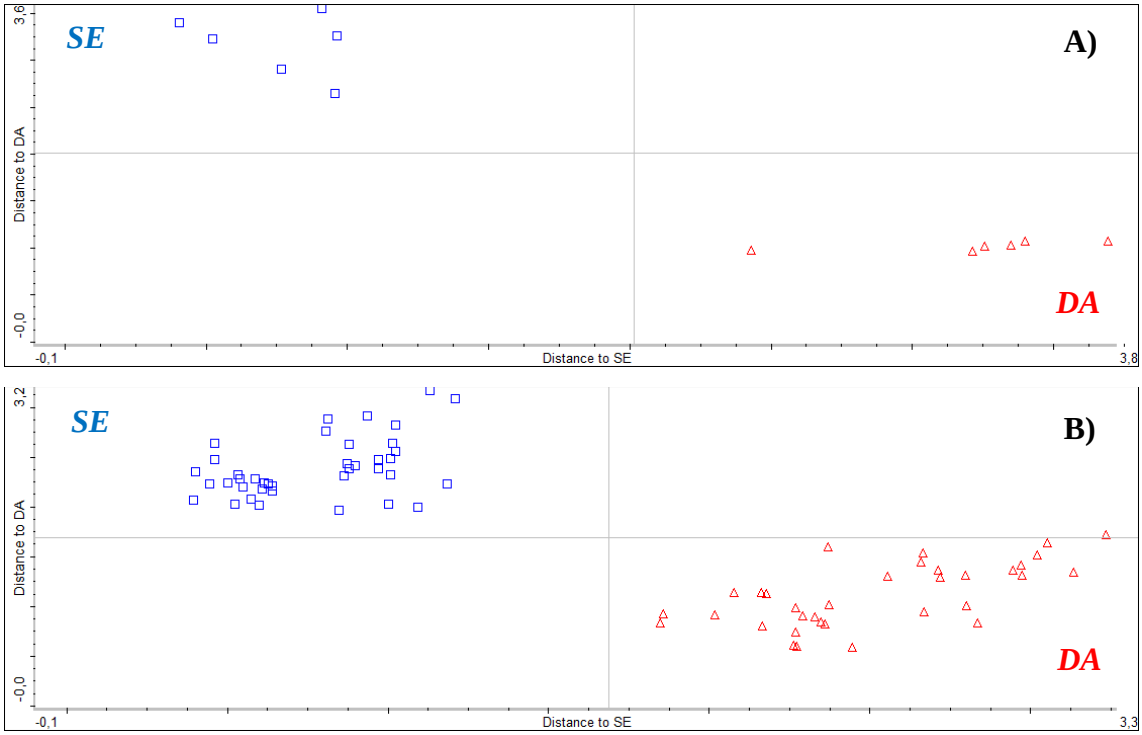

Fig. 25: *Discriminant analysis performed on **A)** PBS solutions **B)** aCSF solutions. The number of analysed samples in PBS is 12, in aCSF 73. Blue squares in the upper left corner signify samples containing higher amount of serotonin, that is ratios 1:5 and 1:10, that were correctly assigned to serotonin, whereas red triangles in the bottom right corner signify samples containing higher amount of dopamine, that is ratios 5:1 and 10:1, correctly assigned to dopamine.*

4.4 Limit of Detection for DA and SE in aCSF

A set of experiments was performed for both dopamine and serotonin dissolved in aCSF in concentration range from 0.1 mM to 1 mM with the intention to fit a linear calibration curve and assess the limit of detection (LOD) for this MA-SERS method. The LOD was calculated as $3\sigma/k$, where σ is the standard deviation of the blank sample at the position of the peak chosen for quantitative analysis, and k is the slope of the linear calibration curve.[81]

For the detection of dopamine, higher number of exposures (64) were used to obtain clearer spectra. The peak at 1485 cm^{-1} was chosen for DA quantification. The fitted linear calibration curve has correlation coefficient R^2 = 0.9964, and the calculated limit of detection for DA is 1.82 μM (Fig. 26).

Regarding serotonin, more variables had to be tuned to assemble the calibration curve. Firstly, higher amount of the sample was mixed with the magnetic composite (50 μL, ratio 1:1), and low laser power with longer expositions were used (1 mW, 128 exposures) for better resolution of the spectra. The peak at 1337 cm^{-1} was chosen for SE quantification. The fitted linear calibration curve has correlation coefficient R^2 = 0.9942, and the calculated limit of detection for SE is 0.04 mM (Fig. 27).

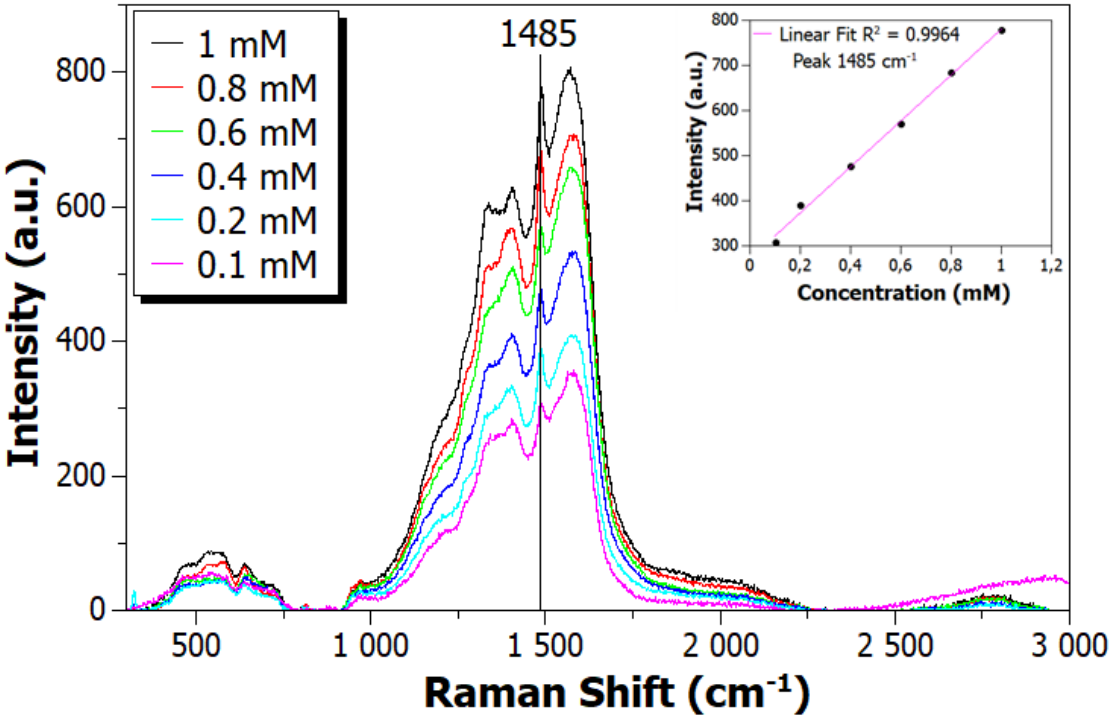

Fig. 26: *MA-SERS spectra of dopamine in aCSF in concentrations 1 mM (black), 0.8 mM (red), 0.6 mM (green), 0.4 mM (blue), 0.2 mM (turquoise), and 0.1 mM (pink). The spectra were obtained with 532 nm excitation wavelength, laser power 4 mW, and 64 exposures. The peak used for quantification is 1487 cm^{-1}. Intensities of this peak are plotted against respective concentrations in the smaller figure in the right corner and fitted with linear equation. Its R^2 value is 0.9964. The LOD calculated from the slope of the linear equation and the standard deviation of blank was 1.82 μM.*

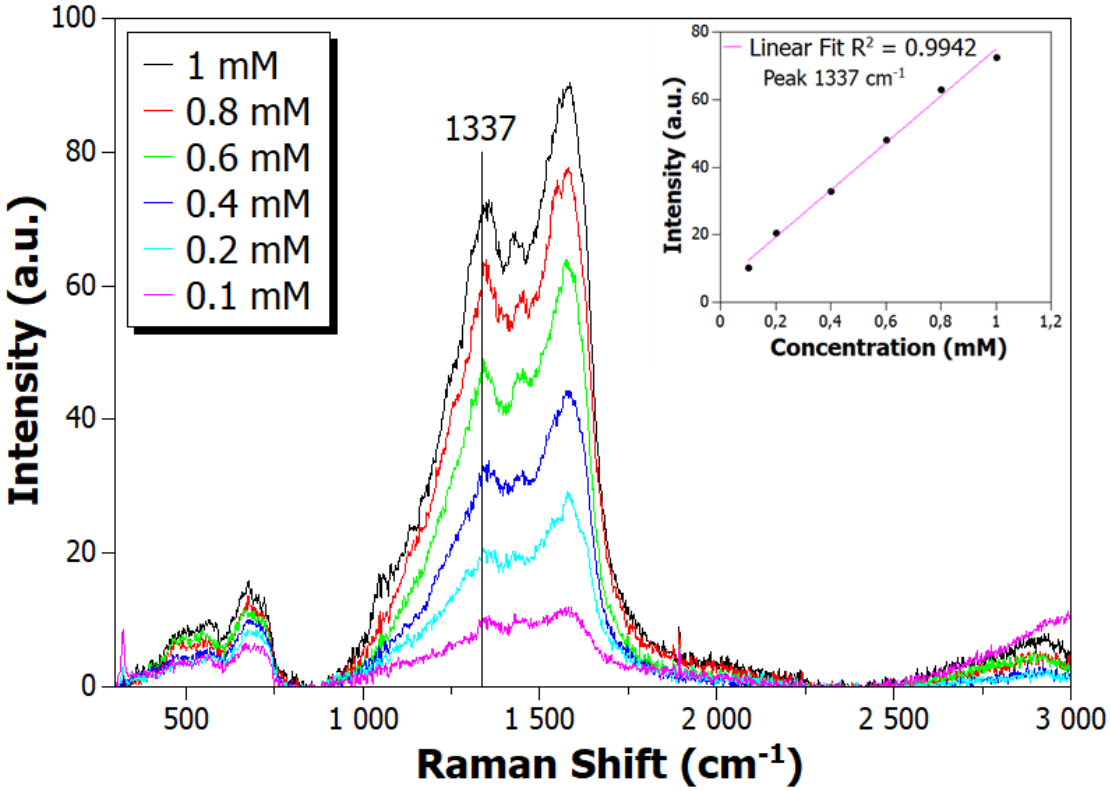

Fig. 27: *MA-SERS spectra of serotonin in aCSF in concentrations 1 mM (black), 0.8 mM (red), 0.6 mM (green), 0.4 mM (blue), 0.2 mM (turquoise), and 0.1 mM (pink). The spectra were obtained with 532 nm excitation wavelength, laser power 1 mW, and 128 exposures. The peak used for quantification is 1337 cm^{-1}. Intensities of this peak are plotted against respective concentrations in the smaller figure in the right corner and fitted with linear equation. Its R^2 value is 0.9942. The LOD calculated from the slope of the linear equation and the standard deviation of blank was 0.04 mM.*

4.5 MA-SERS Detection from Mouse Brain Tissue (Striatum)

Three samples of striatum were used for MA-SERS experiments sensing DA and SE at physiological concentrations (~10^{-9} M) from a brain tissue extract. The clearest spectra were obtained with laser power 1 mW and 128 exposures. The best spectra of each striatum sample, called A, B, and C, are shown in Fig. 28.

The measured signal is more complex than the signal of a mixture of dopamine and serotonin in aCSF. There are more peaks, well defined, which implies more analytes adsorbed onto the composite. However, some of the peaks match those assigned to either dopamine or serotonin in previous experiments. This is shown in a close-up in Fig. 29 which compares striatal peaks with standards of dopamine and serotonin solutions in distilled water. The red vertical lines signify DA peaks and they are at positions 1266,

1271, 1283, 1327, 1348, 1394, 1426, 1485, and 1550 cm^{-1}, whereas green vertical lines signify SE peaks at positions 1307, 1337, 1373, 1384, 1442, 1469, 1553, 1576, and 1594 cm^{-1}. Striatum A (black) has 5 peaks that can be attributed to DA and 5 peaks that can be attributed to SE, striatum B (blue) has 3 and 6 peaks that can be attributed to DA and SE, and striatum C (pink) has 6 and 4 peaks that can be attributed DA and SE, respectively.

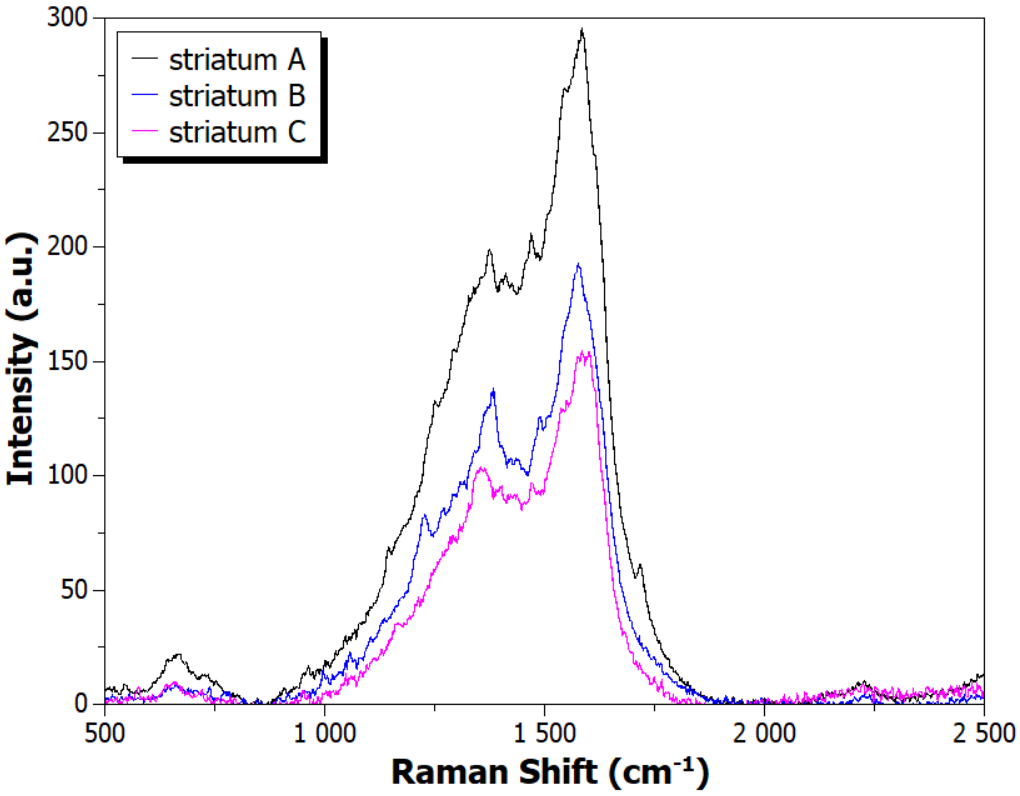

Fig. 28: *MA-SERS spectra of extracts from striatal brain tissue from samples* A *(black),* B *(blue), and* C *(pink). The spectra were obtained with 532 nm excitation wavelength, laser power 1 mW, and 128 exposures.*

Although the LODs calculated from previous experiments were higher than the basal concentration of measured neurotransmitters, it is possible the signal is in fact from dopamine and serotonin, among other biological adsorbates. That is due to the fact that DA and SE are somehow stabilized in their natural environment, possibly protected from partial sample degradation during incubation or the measurement itself.

Such results imply it would be possible to distinguish both dopamine and serotonin in striatal extract in a label-free manner with this magnetic nanocomposite. However, it is necessary to further optimize the method to deem this identification reliable.

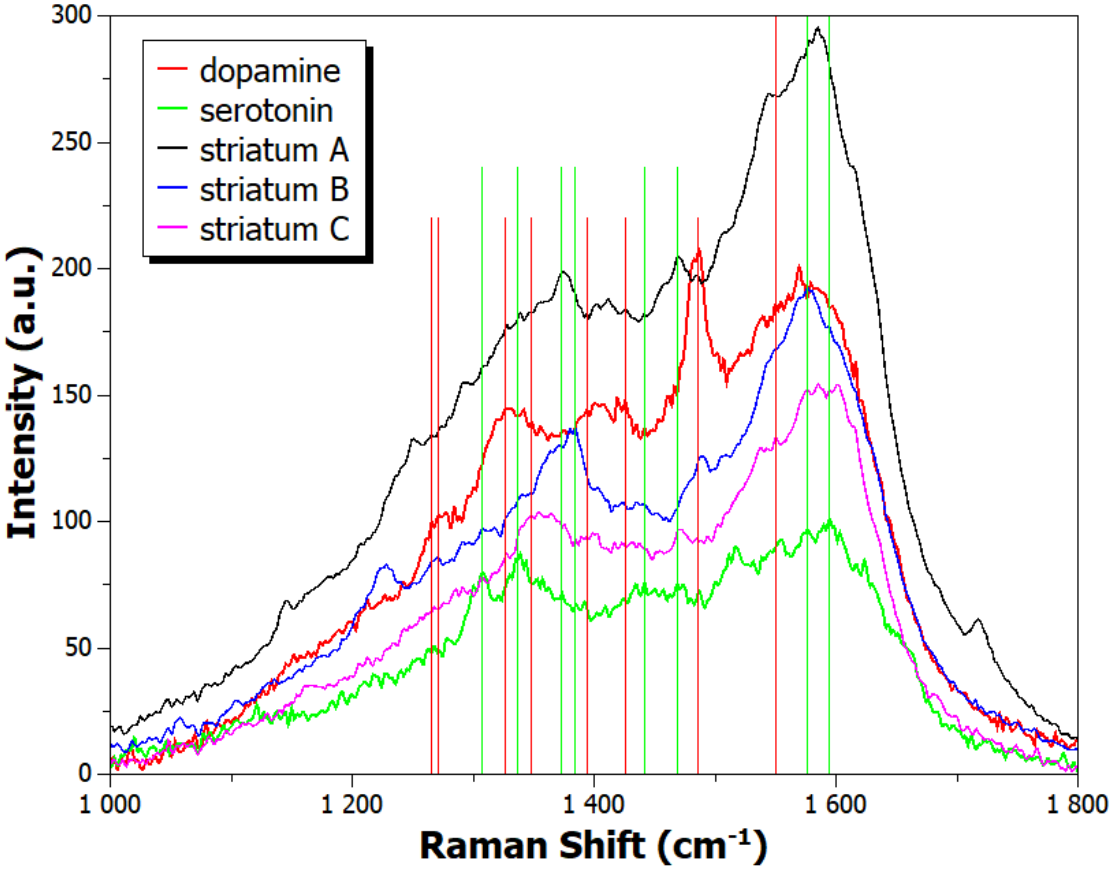

***Fig. 29**: A close-up comparison of striatal spectra* A *(black),* B *(blue), and* C *(pink) with dopamine (red) and serotonin (green) standards in distilled water. The spectra of striatal tissue were obtained with 532 nm excitation wavelength, laser power 1 mW, and 128 exposures. The spectra of standards were obtained with 532 nm excitation wavelength, laser power 4 mW, and 16 exposures.*

Red vertical lines mark matching DA peaks at positions 1266, 1271, 1327, 1348, 1394, 1426, 1485, and 1550 cm^{-1}, and green vertical lines mark matching SE peaks at positions 1307, 1337, 1373, 1384, 1442, 1469, 1576, and 1594 cm^{-1}.

Striatum A *has possible DA peaks at 1266, 1327, 1394, 1426, and 1485 cm^{-1}, and possible SE peaks at 1307, 1337, 1373, 1442, and 1469 cm^{-1}.*

Striatum B *has possible DA peaks at 1271, 1426, and 1485 cm^{-1}, and possible SE peaks at 1307, 1373, 1384, 1442, 1576, and 1594 cm^{-1}.*

And striatum C *has possible DA peaks at 1327, 1348, 1394, 1426, 1485, and 1550 cm^{-1}, and possible SE peaks at 1307, 1384, 1576, and 1594 cm^{-1}.*

5 SUMMARY

In this work, label-free detection of dopamine and serotonin was achieved by applying magnetically assisted surface enhanced Raman spectroscopy (MA-SERS).

Using a magnetic nanocomposite has several advantages over colloid solutions – it simplifies sample separation from a complex matrix, enables sample washing with magnetic decantation, and sample preconcentration before measurements, all by simply applying external magnetic field. Using a magnetic composite also guarantees spatial proximity of signal enhancing AgNPs, which leads to high number of hot spots, therefore better signal enhancement. The composite has a magnetic core composed of magnetite with a small amount of maghemite onto which CMC (carboxymethylcellulose) is adsorbed and AgNPs are immobilized.

Firstly, dopamine and serotonin were sensed separately from three different matrixes. Laser excitation wavelength 532 nm and laser power 4 mW were used. The number of exposures was tuned based on the clarity of measured peaks. Reproducible spectra of both neurotransmitters in distilled water, PBS solution, and artificial cerebrospinal fluid (aCSF) were gathered.

In the following experiments, mixtures of dopamine and serotonin with respective ratios 1:1, 1:5, 5:1, 1:10, and 10:1 in PBS and aCSF were simultaneously detected. By applying discriminant analysis, both neurotransmitters could be distinguished from all mixtures.

Calibration curves of neurotransmitters in aCSF within concentration range 0.1 – 1 mM were assembled with correlation coefficients 0.9964 for DA and 0.9942 for SE. Their limits of detection were calculated. For dopamine, which gave more defined spectra with higher intensity, the LOD was 1.82 μM. For serotonin, whose spectra were more problematic, but still distinguishable, the LOD was 0.04 mM.

Finally, the magnetic nanocomposite was applied for the detection from a biological sample, extract from mouse striatum. The measured signal was more complex than the signal of a mixture of dopamine and serotonin. There were more defined peaks, which implied more analytes adsorbed onto the nanocomposite. However, there were some peaks previously assigned to both dopamine and serotonin. This suggests the magnetic nanocomposite could be used for dopamine and serotonin detection from striatum, after further optimization of the method.

6 ZÁVĚR

V této práci bylo dosaženo detekce dopaminu a serotoninu pomocí metodiky magneticky asistované povrchem zesílené Ramanovy spektroskopie (MA-SERS).

Použití magnetického kompozitu má několik výhod oproti použití koloidního roztoku – kompozit zjednodušuje separaci analytu od komplexní matrice, promývání vzorku magnetickou dekantací, a dovolí zakoncentrovat analyt před měřením, vše jednoduše pomocí aplikace externího magnetického pole. Magnetický kompozit také zajistí prostorovou blízkost signál zesilujících nanočástic stříbra, což vede k vyššímu množství tzv. hot spots a vyššímu zesílení signálu. Tento kompozit má jádro složené z magnetitu a částečně maghemitu, na které je adsorbovaná karboxymethylcelulóza a imobilizované nanočástice stříbra.

Nejprve byly neurotransmitery dopamin a serotonin detekovány samostatně ze tří různých matric. Na experimenty byly použity excitační vlnová délka laseru 532 nm a výkon laseru 4 mW. Počet expozic byl nastavován na základě rozlišení spekter. Reprodukovatelná spektra obou neurotransmiterů byla získána pro vzorky v destilované vodě, PBS pufru a umělého mozkomíšního moku (aCSF).

V následujících experimentech byly simultánně detekovány mixy neurotransmiterů v PBS a aCSF roztocích v poměrech 1:1, 1:5, 5:1, 1:10 a 10:1. Pomocí diskriminační analýzy bylo možno rozlišit oba neurotransmitery ze všech naměřených vzorků.

Dále byly sestavy kalibrační křivky neurotransmiterů v roztoku aCSF v koncentračním rozmezí 0,1 – 1 mM. Hodnota spolehlivosti lineárního fitu pro dopamin byla 0,9964 a pro serotonin 0,9942. Limit detekce použité metody byl pro dopamin (1,82 μM) nižší než pro serotonin (0,04 mM), jak se dalo předpokládat z naměřených spekter. Signál dopaminu měl stabilně vyšší intenzitu a lépe definované peaky než serotonin.

Nakonec byly neurotransmitery dopamin a serotonin detekovány z extraktu striata myší. Získaný signál byl komplexnější než signál mixu neurotransmiterů v aCSF, obsahoval více lépe definovaných peaků, což značí přítomnost dalších analytů naadsorbovaných na kompozitu. Avšak ve spektrech bylo vždy několik peaků, které byly v předchozích experimentech přiřazeny dopaminu nebo serotoninu. To značí, že magnetický nanokompozit by bylo možné po řádném dokončení optimalizace metody aplikovat k detekci neurotransmiterů dopaminu a serotoninu ze striata.

7 BIBLIOGRAPHY

(1) Zhang, A.; Neumeyer, J. L.; Baldessarini, R. J. Recent Progress in Development of Dopamine Receptor Subtype-Selective Agents: Potential Therapeutics for Neurological and Psychiatric Disorders. *Chem. Rev.* **2007**, *107*, 274–302.

(2) Dunlop, B. W.; Nemeroff, C. B. The Role of Dopamine in the Pathophysiology of Depression. *Arch. Gen. Psychiatry* **2007**, *64* (3), 327–337.

(3) Koob, G. F.; Volkow, N. D. Neurocircuitry of Addiction. *Neuropsychopharmacology* **2010**, *35* (1), 217–238.

(4) Huang, L. C.; Lin, S. H.; Tseng, H. H.; Chen, K. C.; Yang, Y. K. The Integrated Model of Glutamate and Dopamine Hypothesis for Schizophrenia: Prediction and Personalized Medicine for Prevent Potential Treatment-Resistant Patients. *Med. Hypotheses* **2020**, *143* (June), 110–159.

(5) Lucki, I. The Spectrum of Behaviors Influenced by Serotonin. *Biol. Psychiatry* **1998**, *44* (3), 151–162.

(6) Mishra, A.; Anand, M.; Umesh, S. Neurobiology of Eating Disorders - an Overview. *Asian J. Psychiatr.* **2017**, *25* (2017), 91–100.

(7) Maron, E.; Nutt, D.; Shlik, J. Neuroimaging of Serotonin System in Anxiety Disorders. *Curr. Pharm. Des.* **2012**, *18* (35), 5699–5708.

(8) El-Sherbeni, A. A.; Stocco, M. R.; Wadji, F. B.; Tyndale, R. F. Addressing the Instability Issue of Dopamine during Microdialysis: The Determination of Dopamine, Serotonin, Methamphetamine and Its Metabolites in Rat Brain. *J. Chromatogr. A* **2020**, *1627*.

(9) Kumar, M.; Wang, M.; Swamy, B. E. K.; Praveen, M.; Zhao, W. Poly (Alanine)/NaOH/MoS2/MWCNTs Modified Carbon Paste Electrode for Simultaneous Detection of Dopamine, Ascorbic Acid, Serotonin and Guanine. *Colloids Surfaces B Biointerfaces* **2020**, *196* (August), 111299.

(10) Vander Ende, E.; Bourgeois, M. R.; Henry, A.-I.; Chávez, J. L.; Krabacher, R.; Schatz, G. C.; Van Duyne, R. P. Physicochemical Trapping of Neurotransmitters in Polymer-Mediated Gold Nanoparticle Aggregates for Surface-Enhanced Raman Spectroscopy. *Anal. Chem.* **2019**, *91* (15), 9554–9562.

(11) Qiu, C.; Bennet, K. E.; Tomshine, J. R.; Hara, S.; Ciubuc, J. D.; Schmidt, U.; Durrer, W. G.; McIntosh, M. B.; Eastman, M.; Manciu, F. S. Ultrasensitive Detection of Neurotransmitters by Surface Enhanced Raman Spectroscopy for Biosensing Applications. *Biointerface Res. Appl. Chem.* **2017**, *7* (1), 1921–1926.

(12) Wang, P.; Xia, M.; Liang, O.; Sun, K.; Cipriano, A. F.; Schroeder, T.; Liu, H.; Xie, Y. H. Label-Free SERS Selective Detection of Dopamine and Serotonin Using Graphene-Au Nanopyramid Heterostructure. *Anal. Chem.* **2015**, *87* (20), 10255–10261.

(13) Phung, V. D.; Kook, J. K.; Koh, D. Y.; Lee, S. W. Hierarchical Au Nanoclusters Electrodeposited on Amine-Terminated ITO Glass as a SERS-Active Substrate for the Reliable and Sensitive Detection of Serotonin in a Tris-HCl Buffer Solution. *Dalt. Trans.* **2019**, *48* (42), 16026–16033.

(14) Do, P. Q. T.; Huong, V. T.; Phuong, N. T. T.; Nguyen, T. H.; Ta, H. K. T.; Ju, H.; Phan, T. B.; Phung, V. D.; Trinh, K. T. L.; Tran, N. H. T. The Highly Sensitive Determination of Serotonin by Using Gold Nanoparticles (Au NPs) with a Localized Surface Plasmon Resonance (LSPR) Absorption Wavelength in the Visible Region. *RSC Adv.* **2020**, *10* (51), 30858–30869.

(15) Manciu, F. S.; Manciu, M.; Ciubuc, J. D.; Sundin, E. M.; Ochoa, K.; Eastman, M.; Durrer, W. G.; Guerrero, J.; Lopez, B.; Subedi, M.; et al. Simultaneous Detection of Dopamine and Serotonin-a Comparative Experimental and Theoretical Study of Neurotransmitter Interactions. *Biosensors* **2019**, *9* (1).

(16) Spitzer, N. C. Neurotransmitter Switching in the Developing and Adult Brain. *Annu. Rev. Neurosci.* **2017**, *40*, 1–19.

(17) Sharaff, F.; Freestone, P. Microbial Endocrinology. *Cent. Eur. J. Biol.* **2011**, *6* (5), 685–694.

(18) Ma, X.; Wang, Z.; Zhang, X. Evolution of Dopamine-Related Systems: Biosynthesis, Degradation and Receptors. *J. Mol. Evol.* **2010**, *71* (5–6), 374–384.

(19) Elsworth, J. D.; Roth, R. H. Dopamine Synthesis, Uptake, Metabolism, and Receptors: Relevance to Gene Therapy of Parkinson's Disease. *Exp. Neurol.* **1997**, *144* (1), 4–9.

(20) Shen, Y.; Ye, M. Y. Determination of the Stability of Dopamine in Aqueous Solutions by High Performance Liquid Chromatography. *J. Liq. Chromatogr.* **1994**, *17* (7), 1557–1565.

(21) Poirier, J.; Donaldson, J.; Barbeau, A. The Specific Vulnerability of the Substantia Nigra to MPTP Is Related to the Presence of Transition Metals. *Biochem. Biophys. Res. Commun.* **1985**, *128* (2), 25–33.

(22) Segura-Aguilar, J.; Paris, I. Mechanisms of Dopamine Oxidation and Parkinson's Disease. *Handb. Neurotox.* **2014**, *1–3*.

(23) Sánchez-Rivera, A. E.; Corona-Avendaño, S.; Alarcón-Angeles, G.; Rojas-Hernández, A.; Ramírez-Silva, M. T.; Romero-Romo, M. A. Spectrophotometric Study on the Stability of Dopamine and the Determination of Its Acidity Constants. *Spectrochim. Acta - Part A Mol. Biomol. Spectrosc.* **2003**, *59* (13), 3193–3203.

(24) Milovanović, B.; Ilić, J.; Stanković, I. M.; Popara, M.; Petković, M.; Etinski, M. A Simulation of Free Radicals Induced Oxidation of Dopamine in Aqueous Solution. *Chem. Phys.* **2019**, *524* (March), 26–30.

(25) Lees, A. J.; Hardy, J.; Revesz, T. Parkinson's Disease. *Lancet* **2009**, *373* (9680), 2055–2066.

(26) Ashok, A. H.; Mizuno, Y.; Volkow, N. D.; Howes, O. D. Association of Stimulant Use with Dopaminergic Alterations in Users of Cocaine, Amphetamine, or Methamphetamine a Systematic Review and Meta-Analysis. *JAMA Psychiatry* **2017**, *74* (5), 511–519.

(27) Howes, O. D.; Kapur, S. The Dopamine Hypothesis of Schizophrenia: Version III - The Final Common Pathway. *Schizophr. Bull.* **2009**, *35* (3), 549–562.

(28) van Os, J.; Kapur, S. Schizophrenia. *Lancet* **2009**, *374* (9690), 635–645.

(29) Spiller, R. Serotonin and GI Clinical Disorders. *Neuropharmacology* **2008**, *55* (6), 1072–1080.

(30) Tyce, G. M. Origin and Metabolism of Serotonin. *J. Cardiovasc. Pharmacol.* **1990**, *16* (Suppl. 3).

(31) O'Mahony, S. M.; Clarke, G.; Borre, Y. E.; Dinan, T. G.; Cryan, J. F. Serotonin, Tryptophan Metabolism and the Brain-Gut-Microbiome Axis. *Behav. Brain Res.* **2015**, *277*, 32–48.

(32) Maruyama, W.; Nakahara, D.; Dostert, P.; Hashiguchi, H.; Ohta, S.; Hirobe, M.; Takahashi, A.; Nagatsu, T.; Naoi, M. Selective Release of Serotonin by Endogenous Alkaloids, 1-Methyl-6,7-Dihydroxy-1,2,3,4-Tetrahydroisoquinolines, (R)- and (S)Salsolinol, in the Rat Striatum; in Vivo Microdialysis Study. *Neurosci. Lett.* **1993**, *149* (2), 115–118.

(33) Li, L.; Lu, Y.; Qian, Z.; Yang, Z.; Yang, K.; Zong, S.; Wang, Z. Ultra-Sensitive Surface Enhanced Raman Spectroscopy Sensor for in-Situ Monitoring of Dopamine Release Using Zipper-like Ortho-Nanodimers. *Biosens. Bioelectron.* **2021**, *180* (February), 113100.

(34) Yang, C.; Hu, K.; Wang, D.; Zubi, Y.; Lee, S. T.; Puthongkham, P.; Mirkin, M. V.; Venton, B. J. Cavity Carbon-Nanopipette Electrodes for Dopamine Detection. *Anal. Chem.* **2019**, *91* (7), 4618–4624.

(35) Schnell, A.; Sandrelli, F.; Ranc, V.; Ripperger, J. A.; Brai, E.; Alberi, L.; Rainer, G.; Albrecht, U. Mice Lacking Circadian Clock Components Display Different Mood-Related Behaviors and Do Not Respond Uniformly to Chronic Lithium Treatment. *Chronobiol. Int.* **2015**, *32* (8), 1075–1089.

(36) Urbanová, V.; Karlický, F.; Matěj, A.; Šembera, F.; Janoušek, Z.; Perman, J. A.; Ranc, V.; Čépe, K.; Michl, J.; Otyepka, M.; et al. Fluorinated Graphenes as Advanced Biosensors-Effect of Fluorine Coverage on Electron Transfer Properties and Adsorption of Biomolecules. *Nanoscale* **2016**, *8* (24), 12134–12142.

(37) Nie, S.; Emory, S. R. Probing Single Molecules and Single Nanoparticles by Surface-Enhanced Raman Scattering. *Science (80-.).* **1997**, *275* (5303), 1102–1106.

(38) Smith, E.; Dent, G. *Modern Raman Spectroscopy A Practical Approach*; John Wiley & Sons Ltd, **2005**.

(39) D. Dzebo. Photon Upconversion through Triplet-Triplet Annihilation Towards Higher Efficiency and Solid State Applications, CHALMERS UNIVERSITY OF TECHNOLOGY, Goteborg, Sweden, **2016**.

(40) Moskovits, M. Surface-Enhanced Raman Spectroscopy: A Brief Retrospective. *J. Raman Spectrosc.* **2005**, *36* (6–7), 485–496.

(41) Tian, F.; Bonnier, F.; Casey, A.; Shanahan, A. E.; Byrne, H. J. Surface Enhanced Raman Scattering with Gold Nanoparticles: Effect of Particle Shape. *Anal. Methods* **2014**, *6* (22), 9116–9123.

(42) Jeong, D. H.; Zhang, Y. X.; Moskovits, M. Polarized Surface Enhanced Raman Scattering from Aligned Silver Nanowire Rafts. *J. Phys. Chem. B* **2004**, *108* (34), 12724–12728.

(43) Stiles, P. L.; Dieringer, J. A.; Shah, N. C.; Van Duyne, R. P. Surface-Enhanced Raman Spectroscopy. *Annu. Rev. Anal. Chem* **2008**, *1*, 601–626.

(44) Wang, J.; Lin, D.; Lin, J.; Yu, Y.; Huang, Z.; Chen, Y.; Lin, J.; Feng, S.; Li, B.; Liu, N.; et al. Label-Free Detection of Serum Proteins Using Surface-Enhanced Raman Spectroscopy for Colorectal Cancer Screening. *J. Biomed. Opt.* **2014**, *19* (8), 087003.

(45) Phung, V. D.; Jung, W. S.; Nguyen, T. A.; Kim, J. H.; Lee, S. W. Reliable and Quantitative SERS Detection of Dopamine Levels in Human Blood Plasma Using a Plasmonic Au/Ag Nanocluster Substrate. *Nanoscale* **2018**, *10* (47), 22493–22503.

(46) Ranc, V.; Markova, Z.; Hajduch, M.; Prucek, R.; Kvitek, L.; Kaslik, J.; Safarova, K.; Zboril, R. Magnetically Assisted Surface-Enhanced Raman Scattering Selective Determination of Dopamine in an Artificial Cerebrospinal Fluid and a Mouse Striatum Using Fe3O4/Ag Nanocomposite. *Anal. Chem.* **2014**, *86* (6), 2939–2946.

(47) Ranc, V.; Žižka, R.; Chaloupková, Z.; Ševčík, J.; Zbořil, R. Imaging of Growth Factors on a Human Tooth Root Canal by Surface-Enhanced Raman Spectroscopy. *Anal. Bioanal. Chem.* **2018**, *410* (27), 7113–7120.

(48) Wang, J.; Wu, X.; Wang, C.; Shao, N.; Dong, P.; Xiao, R.; Wang, S. Magnetically Assisted Surface-Enhanced Raman Spectroscopy for the Detection of Staphylococcus Aureus Based on Aptamer Recognition. *ACS Appl. Mater. Interfaces* **2015**, *7* (37), 20919–20929.

(49) Kumamoto, Y.; Harada, Y.; Takamatsu, T.; Tanaka, H. Label-Free Molecular Imaging and Analysis by Raman Spectroscopy. *Japan Soc. Histochem. Cytochem.* **2018**, *51* (3), 101–110.

(50) Vo, V. T.; Gwon, Y.; Duc, V.; Don, Y.; Jong, S.; Kim, H.; Lee, S. W. Ag-Deposited Porous Silicon as a SERS - Active Substrate for the Sensitive Detection of Catecholamine Neurotransmitters. *Electron. Mater. Lett.* **2021**, *17*, 292–298.

(51) Moody, A. S.; Sharma, B. Multi-Metal, Multi-Wavelength Surface-Enhanced Raman Spectroscopy Detection of Neurotransmitters. *ACS Chem. Neurosci.* **2018**, *9* (6), 1380–1387.

(52) Dumont, E.; De Bleye, C.; Cailletaud, J.; Sacré, P. Y.; Van Lerberghe, P. B.; Rogister, B.; Rance, G. A.; Aylott, J. W.; Hubert, P.; Ziemons, E. Development of a SERS Strategy to Overcome the Nanoparticle Stabilisation Effect in Serum-Containing Samples: Application to the Quantification of Dopamine in the Culture Medium of PC-12 Cells. *Talanta* **2018**, *186*, 8–16.

(53) Moody, A. S.; Payne, T. D.; Barth, A.; Sharma, B. Surface-Enhanced Spatially-Offset Raman Spectroscopy (SESORS) for Detection of Neurochemicals through the Skull at Physiologically Relevant Concentrations. *R. Soc. Chem.* **2020**, *145*, 1885–1893.

(54) Phung, V. D.; Sik, J. W.; Kim, J.; Lee, S. Au Nanostructures Electrodeposited on Graphene Oxide-Modified ITO Glass as SERS Substrates for Dopamine Detection in Human Serum. In *22nd Microoptics Conference (MOC)*; **2017**.

(55) Bailey, M. R.; Martin, R. S.; Schultz, Z. D. Role of Surface Adsorption in the Surface-Enhanced Raman Scattering and Electrochemical Detection of Neurotransmitters. *J. Phys. Chem. C* **2016**, *120* (37), 20624–20633.

(56) Lussier, F.; Brulé, T.; Bourque, M. J.; Ducrot, C.; Trudeau, L. É.; Masson, J. F. Dynamic SERS Nanosensor for Neurotransmitter Sensing near Neurons. *Faraday Discuss.* **2017**, *205*, 387–407.

(57) Neri, G.; Fazio, E.; Mineo, P. G.; Scala, A.; Piperno, A. SERS Sensing Properties of New Graphene/Gold Nanocomposite. *Nanomaterials* **2019**, *9* (9), 1–13.

(58) Tezcan, T.; Hsu, C. H. High-Sensitivity SERS Based Sensing on the Labeling Side of Glass Slides Using Low Branched Gold Nanoparticles Prepared with Surfactant-Free Synthesis. *RSC Adv.* **2020**, *10* (56), 34290–34298.

(59) Lee, W.; Kang, B. H.; Yang, H.; Park, M.; Kwak, J. H.; Chung, T.; Jeong, Y.; Kim, B. K.; Jeong, K. H. Spread Spectrum SERS Allows Label-Free Detection of Attomolar Neurotransmitters. *Nat. Commun.* **2021**, *12* (1).

(60) Lim, J. W.; Kang, I. J. Fabrication of Chitosan-Gold Nanocomposites Combined with Optical Fiber as SERS Substrates to Detect Dopamine Molecules. *Bull. Korean Chem. Soc.* **2014**, *35* (1), 25–29.

(61) An, J. H.; Choi, D. K.; Lee, K. J.; Choi, J. W. Surface-Enhanced Raman Spectroscopy Detection of Dopamine by DNA Targeting Amplification Assay in Parkisons's Model. *Biosens. Bioelectron.* **2015**, *67*, 739–746.

(62) Luo, Y.; Ma, L.; Zhang, X.; Liang, A.; Jiang, Z. SERS Detection of Dopamine Using Label-Free Acridine Red as Molecular Probe in Reduced Graphene Oxide/Silver Nanotriangle Sol Substrate. *Nanoscale Res. Lett.* **2015**, *10* (1).

(63) Figueiredo, M. L. B.; Martin, C. S.; Furini, L. N.; Rubira, R. J. G.; Batagin-Neto, A.; Alessio, P.; Constantino, C. J. L. Surface-Enhanced Raman Scattering for Dopamine in Ag Colloid: Adsorption Mechanism and Detection in the Presence of Interfering Species. *Appl. Surf. Sci.* **2020**, *522* (April), 146–466.

(64) Jiang, Z.; Gao, P.; Yang, L.; Huang, C.; Li, Y. Facile in Situ Synthesis of Silver Nanoparticles on the Surface of Metal-Organic Framework for Ultrasensitive Surface-Enhanced Raman Scattering Detection of Dopamine. *Anal. Chem.* **2015**, *87* (24), 12177–12182.

(65) Liu, R.; Jiang, L.; Yu, Z.; Jing, X.; Liang, X.; Wang, D.; Yang, B.; Lu, C.; Zhou, W.; Jin, S. MXene (Ti3C2Tx)-Ag Nanocomplex as Efficient and Quantitative SERS Biosensor Platform by in-Situ PDDA Electrostatic Self-Assembly Synthesis Strategy. *Sensors Actuators B. Chem.* **2021**, *333* (February), 129581.

(66) Yang, Z.; Liu, T.; Wang, W.; Zhang, L. Stacked Hexagonal Prism of Ag@Ni-MOF-1 as Functionalized SERS Platform through Rational Integration of Catalytic Synthesis of Dopamine-Quinone at Physiological PH with a Biomimetic Route. *Chem. Commun.* **2020**, *56* (20), 3065–3068.

(67) Bu, Y.; Lee, S. W. The Characteristic Agcore-Aushell Nanoparticles as Sers Substrates in Detecting Dopamine Molecules at Various PH Ranges. *Int. J. Nanomedicine* **2015**, *10*, 47–54.

(68) Tang, L.; Li, S.; Han, F.; Liu, L.; Xu, L.; Ma, W.; Kuang, H.; Li, A.; Wang, L.;

Xu, C. SERS-Active Au@Ag Nanorod Dimers for Ultrasensitive Dopamine Detection. *Biosens. Bioelectron.* **2015**, *71*, 7–12.

(69) Moody, A. S.; Baghernejad, P. C.; Webb, K. R.; Sharma, B. Surface Enhanced Spatially Offset Raman Spectroscopy Detection of Neurochemicals Through the Skull. *Anal. Chem.* **2017**, *89* (11), 5688–5692.

(70) Ashley, M. J.; Bourgeois, M. R.; Murthy, R. R.; Laramy, C. R.; Ross, M. B.; Naik, R. R.; Schatz, G. C.; Mirkin, C. A. Shape and Size Control of Substrate-Grown Gold Nanoparticles for Surface-Enhanced Raman Spectroscopy Detection of Chemical Analytes. *J. Phys. Chem. C* **2018**, *122* (4), 2307–2314.

(71) Song, P.; Guo, X.; Pan, Y.; Wen, Y.; Zhang, Z.; Yang, H. SERS and in Situ SERS Spectroelectrochemical Investigations of Serotonin Monolayers at a Silver Electrode. *J. Electroanal. Chem.* **2013**, *688*, 384–391.

(72) Rochefort, A.; Wuest, J. D. Interaction of Substituted Aromatic Compounds with Graphene. *Langmuir* **2009**, *25* (1), 210–215.

(73) Xu, W.; Ling, X.; Xiao, J.; Dresselhaus, M. S.; Kong, J.; Xu, H.; Liu, Z.; Zhang, J. Surface Enhanced Raman Spectroscopy on a Flat Graphene Surface. *Proc. Natl. Acad. Sci. U. S. A.* **2012**, *109* (24), 9281–9286.

(74) Chaloupková, Z.; Balzerová, A.; Bařinková, J.; Medříková, Z.; Šácha, P.; Beneš, P.; Ranc, V.; Konvalinka, J.; Zbořil, R. Label-Free Determination of Prostate Specific Membrane Antigen in Human Whole Blood at Nanomolar Levels by Magnetically Assisted Surface Enhanced Raman Spectroscopy. *Anal. Chim. Acta* **2018**, *997*, 44–51.

(75) Chaloupková, Z.; Balzerová, A.; Medříková, Z.; Srovnal, J.; Hajdúch, M.; Čépe, K.; Ranc, V.; Zbořil, R. Label-Free Determination and Multiplex Analysis of DNA and RNA in Tumor Tissues. *Appl. Mater. Today* **2018**, *12*, 85–91.

(76) Balzerova, A.; Fargasova, A.; Markova, Z.; Ranc, V.; Zboril, R. Magnetically-Assisted Surface Enhanced Raman Spectroscopy (MA-SERS) for Label-Free Determination of Human Immunoglobulin g (IgG) in Blood Using Fe3O4@Ag Nanocomposite. *Anal. Chem.* **2014**, *86* (22), 11107–11114.

(77) Marková, Z.; Šišková, K.; Filip, J.; Šafářová, K.; Prucek, R.; Panáček, A.; Kolář, M.; Zbořil, R. Chitosan-Based Synthesis of Magnetically-Driven Nanocomposites with Biogenic Magnetite Core, Controlled Silver Size, and High Antimicrobial Activity. *Green Chem.* **2012**, *14* (9), 2550–2558.

(78) Massart, R. Preparation of Aqueous Magnetic Liquids in Alkaline and Acidic Media. *IEEE Trans. Magn.* **1981**, *17* (2), 1247–1248.

(79) Griffith, H. Artificial Cerebrospinal-Fluid for Use in Neurosurgery. *J. Neurol. Neurosurg. Psychiatry* **1987**, *50*, 646.

(80) Tu, Q.; Eisen, J.; Chang, C. Surface-Enhanced Raman Spectroscopy Study of Indolic Molecules Adsorbed on Gold Colloids. *J. Biomed. Opt.* **2010**, *15* (2), 020512.

(81) Shi, Y.; Pang, Y.; Huang, N.; Sun, C.; Pan, Y.; Cheng, Y.; Long, Y.; Zheng, H. Competitive Method for Fluorescent Dopamine Detection in Cerebrospinal Fluid Based on the Peroxidase-like Activity of Ficin. *Spectrochim. Acta - Part A Mol.*

Biomol. Spectrosc. **2019**, *209*, 8–13.

(82) Lewis, A. T.; Gaifulina, R.; Isabelle, M.; Dorney, J.; Woods, M. L.; Lloyd, G. R.; Lau, K.; Rodriguez-justo, M.; Kendall, C.; Thomas, G. M. Mirrored Stainless Steel Substrate Provides Improved Signal for Raman Spectroscopy of Tissue and Cells. *J. Raman Spectrosc.* **2016**, *July*.

8 APPENDICES

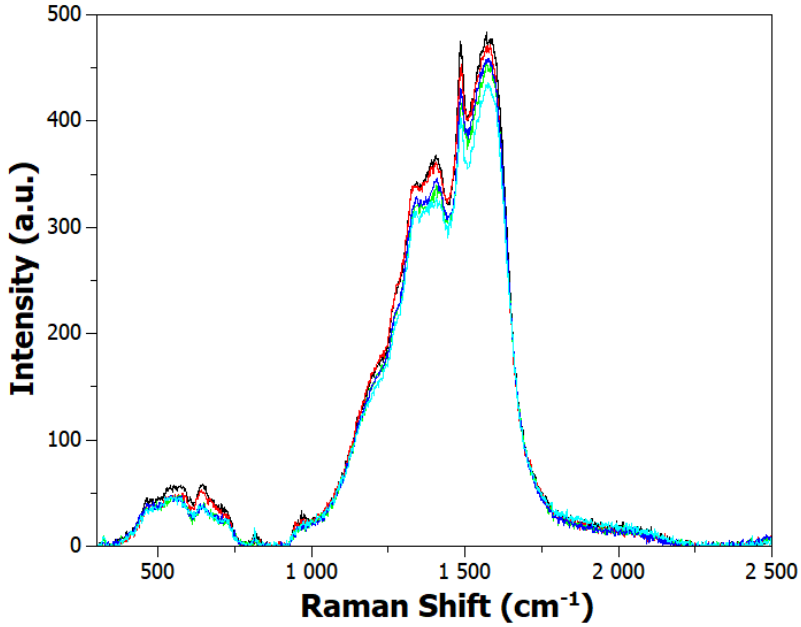

Fig. A1: *Five nearly identical spectra of dopamine in aCSF (10^{-3} M) demonstrating data reproducibility. Spectra were obtained with 532 nm excitation wavelength, laser power 4 mW, and 32 exposures.*

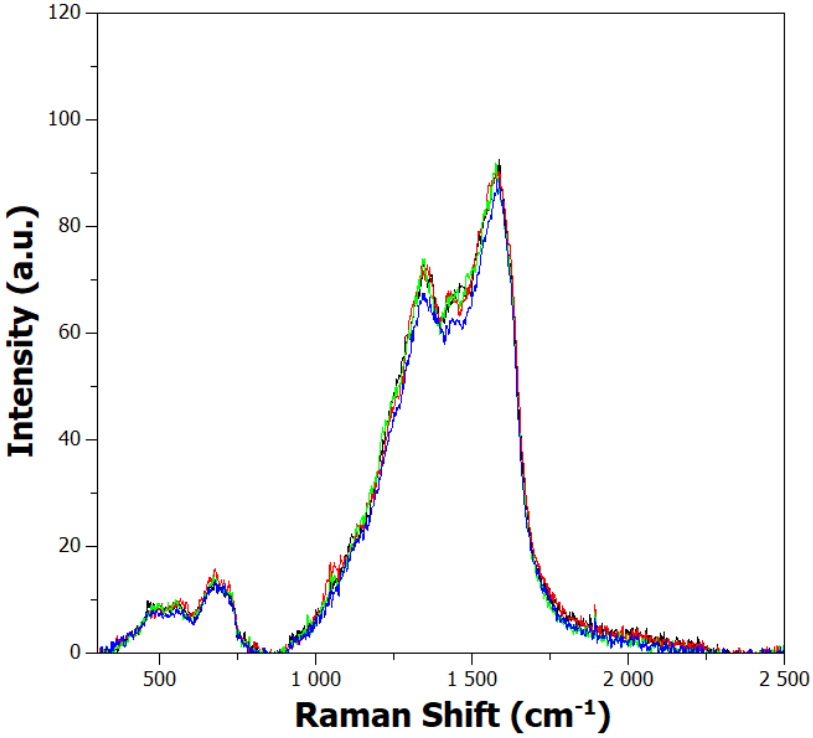

Fig. A2: *Four nearly identical spectra of serotonin in aCSF (10^{-3} M) demonstrating data reproducibility. Spectra were obtained with 532 nm excitation wavelength, laser power 1 mW, and 128 exposures.*

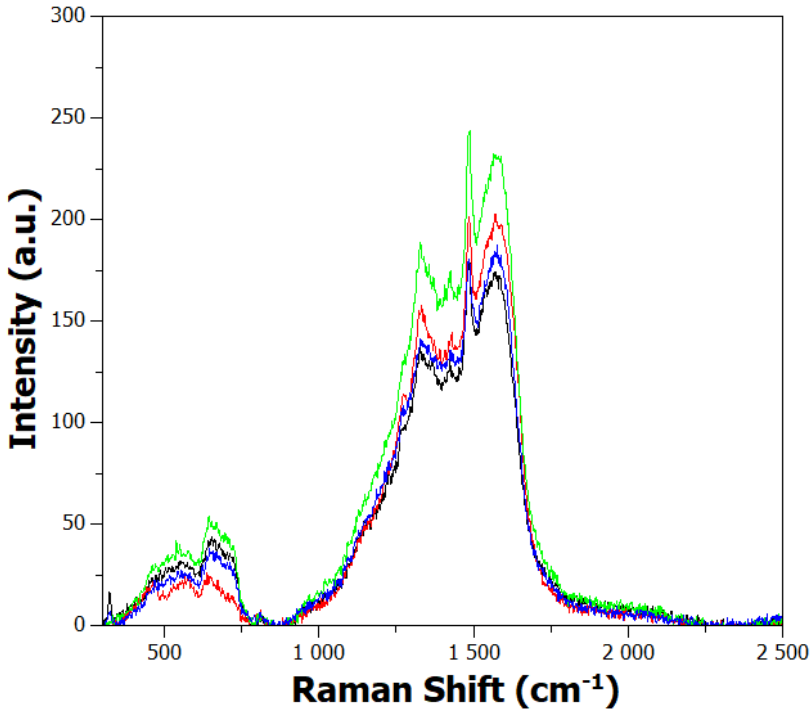

Fig. A3: *Four nearly identical spectra of dopamine:serotonin 1:1 ratio in PBS (10^{-3} M) demonstrating data reproducibility. Spectra were obtained with 532 nm excitation wavelength, laser power 4 mW, and 32 exposures.*

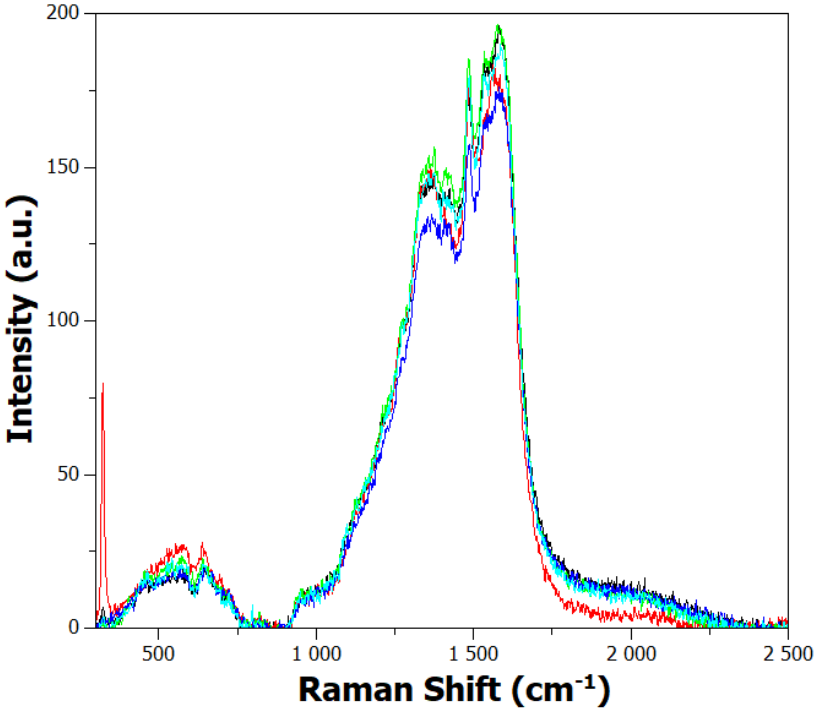

Fig. A4: *Five nearly identical spectra of dopamine:serotonin 1:1 ratio in aCSF (10^{-3} M) demonstrating data reproducibility. Spectra were obtained with 532 nm excitation wavelength, laser power 4 mW, and 32 exposures.*

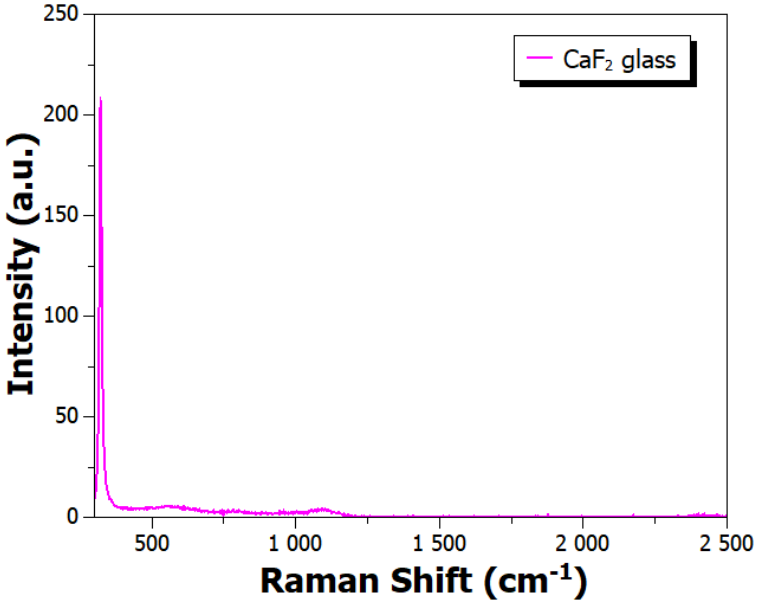

***Fig. A5**: Raman spectrum of the CaF_2 glass platform measured with laser excitation wavelength 532 nm, laser power 4 mW, and 128 exposure. There is one distinguishable peak at 321 cm^{-1}.*[82]

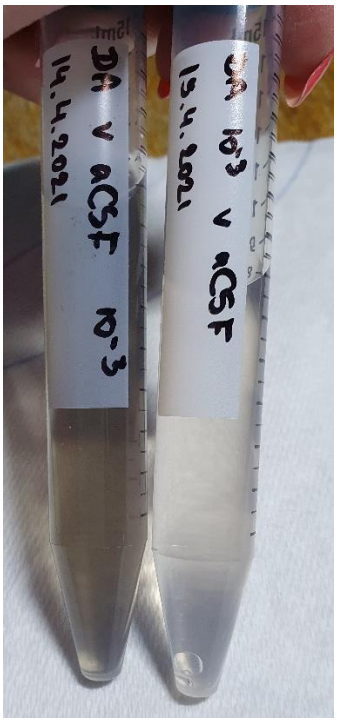

***Fig. A6:** Photo of dopamine solutions (10^{-3} M) in aCSF prepared 24 hours apart, showing dopamine's quick degradation. The grey solution on the left is around 24 hours older than the fresh clear solution on the right that was prepared minutes before taking this picture.*

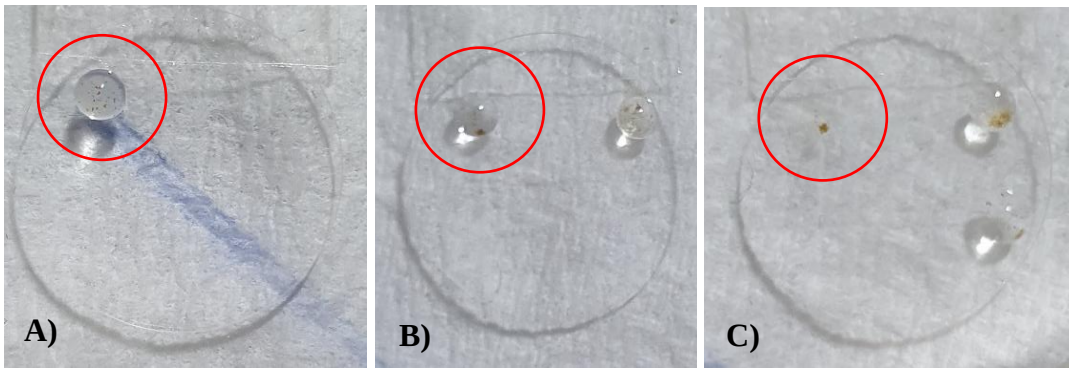

Fig. A7: *Photos showing magnetic preconcentration of a sample before measurents. In* ***A)*** *there is a 2 µL drop of the sample mixed with magnetic nanocomposite (MNP) on* CaF_2 *glass, in* ***B)*** *the sample adsorbed onto the composite is magnetically gathered on the edge, and in* ***C)*** *the dried sample can be seen. This drop comes from striatum analysis – 10 µL of MNP + 2 µL of extracted sample.*